POLITECNICO DI TORINO

Master Degree course in Mechatronic Engineering

Master Degree Thesis

Modelling and simulation of an hydraulic interconnected suspension: analysis of vertical and roll characteristic

Supervisors
Prof. Enrico GALVAGNO

Candidate
Luca TERMINI

ACADEMIC YEAR 2021-2022

Acknowledgements

I would like to thank "Manifattura Automobili Torino" for the opportunity granted, my company tutor Luca Martino for the time and dedicated knowledge and my supervisor, Enrico Galvagno, for the patience and support provided in recent months. A big thank you also goes to my roommates for the patience shown and the support given, to my friends and classmates who have accompanied me in these years of university, and to all the fantastic people I met who shared a piece of their lives. Finally, the biggest thanks goes to my family, who supported me without ever making me lack their affection and their trust. It wouldn't have been the same without you.

Abstract

In literature there are several options for active and semi-active suspensions able to perform height adjustment and damping characteristic control, but very few examples of suspension systems capable of performing the mentioned functions and controlling the car's roll behaviour. One possible alternative is represented by a system that replaces the canonical anti-roll bar, using an interconnected hydraulic circuit. The whole system is composed of an active suspension able to lift the car's body and a hydraulic interconnected circuit which replaces the shock absorber and able to change the damping characteristic controlling the internal active valves. The main object of this project is to study and understand the vertical and rolling behaviour of the car, starting from the company request in terms of vertical and rolling stiffness and to analyze the damping characteristics of the car, by designing and optimizing the hydraulic circuit of the suspension system. In order to achieve these results, a new model of the suspension scheme, using a Simulink toolbox called Multibody to model the mechanical part and the Simscape library to recreate the hydraulic circuit. Once the physical model was created, it was possible to study the kinematic characteristic of the scheme and its role in the dynamic behaviour of the system. Eventually, several and different tests were performed to analyze the stiffness and damping characteristics of the suspension. The results showed a good response in the vertical and lateral direction, proving that the system discussed fulfils the vertical stiffness request given by the company and, in addition, provides good results in terms of rolling behaviour. Same considerations can be made for the damping characteristic, which showed decent results in vertical analysis while, though it seemed to be less performing, in the roll behaviour. According to the results of the analysis, future studies can be carried out to optimize and improve the dynamic behaviour of the car, starting by choosing different hydraulic components or varying the suspension scheme.

Contents

Chapter 1

Active, semi-active suspension and anti-rollbar system. State of the art

1.1 Introduction

This chapter explains the state of the art of active and semi-active suspension in the automotive sector, with an insight into roll control. In mechanics, suspension is a particular system of devices and mechanical parts used in vehicles to reduce and absorb the irregularities of the road, increase comfort and improve the handling characteristic of a vehicle. A schematic system of a car's suspension is composed of: bearing components, primary and secondary elastic members and damping members. While the bearing components are used to link the wheels of the vehicle to the body and guarantee the correct positioning with respect to the reference system of the body, the primary elastic member (springs, roll bar, stop spring) are used to store the energy produced by uneven road profile that the damper element will dissipate. Secondary elastic members are elastic bushings on linkage joints related to the elasto-kinematic behaviour of the suspension and its comfort properties.
While in passive suspensions, the spring stiffness and the damping characteristic of the shock absorber are predefined, in active and semi-active suspension, some characteristics of the system can be changed, for example, is possible to tune the damping behaviour or the ride of the suspension by adding some energy to the system.

The electronically controlled suspension can be classified according to two features:

- Energy input: small energy required means that the system is semi active, high energy instead means active.

- Bandwidth: the characteristic of the suspension can be changed with a specific reaction time.

It is possible to distinguish five different electronic controlled suspensions: three active suspensions (load levelling, slow active and fully active) and two semi-active (adaptive and semi-active). Currently, the most used technology combines load levelling and semi-active damper. [10]

- **Adaptive**: the system is characterized by slow modulation. Since a very small energy (5-10 W) is introduced the bandwidth is limited a few Hz. The stiffness characteristic is not influenced by the system, on the contrary, the damping value of the shock absorber is modulated.

- **semi-active**: the system has higher bandwidth with respect to the adaptive suspensions(30-40 Hz) and a low power demand.

- **load leveling**: fist example of active suspensions since the control strategy changes the working point of the springs . The Bandwidth of the Load-levelling suspensions is very low (0.1-1 Hz) but the energy introduced into the system is some hundred of Watts

- **Slow-active**: The bandwidth is limited to a few Hz, while the power demand of the system is high (1-2 Kw). The passive suspension's device is replaced by an actuator, controlled by the input force of the suspension. The presented system controls both damping and spring characteristic

- **Fully-active**: similar to the slow-active, with the exception that the system reacts very quickly, the bandwidth is very high (30-40 Hz). Also in this case, since the controllability range is beyond the passivity constraint, the power demand is very high (5-10-KW). The presented system controls both damping and spring characteristic

1.2 Semi-active suspensions

The technology is widely used in vast applications, mainly as a primary suspension system but also in large vehicle chassis, where the cabin is separated from the rest of the vehicle and in the cabin-to-seat layer. Semi-active suspension can change the damping coefficient of the shock absorber with low power demand, in this way is possible to change the dynamic behaviour of the vehicle depending on the road conditions or the driving situations.This technology has several advantages:

- **Low power demand** : To change the shock absorber's damping coefficient, the system requires only a few Watts to modify the hydraulic orifices or the viscosity of the fluid.

- **Stability of the system**: since the device is dissipative, stability is guaranteed.

- **High performance**: The adjustable damping ratio guarantees to choose the perfect trade-off between road-holding performances and comfort, depending on the driving conditions.

- **Low weight and low cost** The main damping control technologies can be produced with compact size and low cost for large production volumes.

Semi-active systems consist of dampers capable of varying their damping characteristic with a bandwidth of 20-30Hz; three different shock absorber technologies carry out such a fast actuation: electrohydraulic, magnetorheological and electrorheological dampers. Electrohydraulic damper (EH Dampers)differs from the passive element, since it comprises electronic valves instead of passive ones. The damping characteristic of the system is controlled by changing the section of the valve. The magnetorheological system exploits the creation of a magnetic field to change the viscosity of a magnetorheological fluid. This fluid consists of silicon oil and an iron particle sensitive to the change of the magnetic field.

Similarly to the previous components, the electrorheological system exploits the same principles to adjust the suspension's damping characteristic. The fluid in the cylinder has micron-sized particles which react to the external electric field. If the electric field is absent the piston moves freely inside the cylinder, however, if the electric field differs from zero, particles react as dipoles and the fluid flowing becomes viscoplastic.

The cited technologies are still evolving, other solutions will appear in the future. One of them is the air damping suspensions, consisting of a single device equipped with a piston with variable orifices. The system mixes the damping and elastic behaviour of gases. Another solution is the introduction of electric motors used as dampers with the function of exploiting the energy dissipated.

1.3 Active suspensions: height adjustable systems

The following section is an insight into the active height-adjustable suspension system. In comparison, the semi-active suspension is only able to change the damping force of the shock absorber, the active suspension uses several types of actuators to change the suspension's ride, which means an increase in the car's height. For what may concern the active suspension, the system can be actuated in several ways, like, for examples: pneumatic, hydro-pneumatic, hydraulic and electromechanical actuators.

1.3.1 Pneumatic

This technology is mainly used in public transportation buses, premium cars and high-duty vehicles. The ride height adjustment is performed by pumping air into or out of the air spring bag [7]. This system is composed by:

- Air spring (reinforced rubber bag)
- Air compressor
- Air dryer
- Control system (valves, sensors)

In addition, the pneumatic configuration can adjust the spring rate of the suspension and the damping force. It is implemented by several car companies such as:

- Toyota uses its own system to achieve better performance by lowering the car at high speed for better stability or, similarly, increasing the vehicle's height in rough road conditions [4]. It is composed of an ECU for control strategies, sensors that detect suspension stroke and the difference between the vehicle body and steering shaft, a compressor, height control valve, air chamber and shock absorber.
- FIAT-Chrysler implemented "Quadra-lift": five different height configurations are used to allow an easy entry/exit of the passengers, lower the car at high speed to reduce drag and overcome obstacles in off-road conditions.
- BMW uses self-levelling suspension [7]. When the vehicle loading conditions change, the vehicle height is restored by pumping air to the rear axle. Two different electrical compressors work independently from each other, allowing actuation on the right and left sides of the car.

Pneumatic suspension systems are widely used thanks to the possibility of several adjustments of the spring rate. The main drawbacks are its high cost and reduced reliability, leading to frequent maintenance.

1.3.2 Hydro-pneumatic

Citroen developed this system in the 1950s, schematized in figure 1.3.2(Reproduced from $https://commons.wikimedia.org/wiki/File:Sus_hydropneumatic_english.png$) but it's still used on the company's premium models; it combines hydraulic and pneumatic elements [12]. The hydraulic part of the system is responsible for providing the proper damping force and is also used for height adjustment, while the

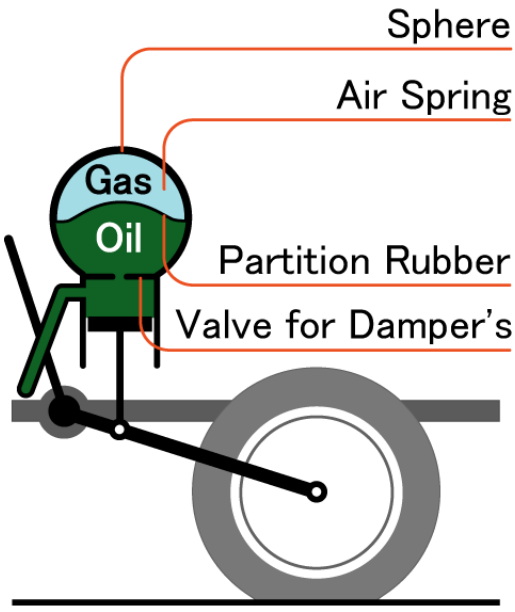

Figure 1.1. Citroen suspension system

pneumatic part is mainly used to change the elastic properties of the suspension. In Citroen's system, a hydropneumatic suspension with a single-acting cylinder and accumulator are directly mounted on them. The suspension cylinder is hydraulically connected so the roll stability is given by the mechanical stabilization bar mounted on the rear and front axle. Another similar system is the one developed by Sarel F. van der Westhuizen and Pieter S. Els called "4s4" (4 state semi-active suspension system) [15], optimized to obtain two different configurations: one for comfort (soft spring and low damping) and one for high handling performance (stiff spring and high damping). This system allows a very fast actuation (<100ms) and it is driven automatically by sensing the vertical acceleration on the vehicle body. The system is composed of two different accumulators:

- 0.1 l accumulator is enabled for stiffer spring
- 0.4 l accumulator for softer spring

Each accumulator is fed by a two-state valve and a damper mounted in parallel; this allows to control the damping characteristic of the suspension. Summarizing the pros and cons, hydro-pneumatic suspensions allow fast height adjustment speed, high reliability and compact size but with high costs.

1.3.3 Hydraulic

Hydraulic height adjustment is composed of linear or rotary actuators, a hydraulic pump, pipes and hydraulic fluid, control valves and sensors. The hydraulic pump injects fluid, up to 200 ba, into the cylinder's upper plate, the increasing pressure moves the upper plate allowing to modify the height of the car. Moreover, the presence of an accumulator guarantees a faster actuation. A scheme of the system is shown in figure 1.3.3 (taken from [7])) For example, Hyundai developed a vehicle height shock absorber [6] (shown in figure 1.3.3, taken from [6]) with a monotube-type cylinder configuration. This shock absorber includes an oil pump per hydraulic pressure, an oil accumulator and a solenoid valve connected with a spool that a controller actuates. The return pipelines are connected with the upper and lower chamber of the cylinder with a solenoid valve. When the control logic selects one of the two states, the accumulator connected with the oil pump is able to actuate the spool and the oil is delivered in one of the two chambers.

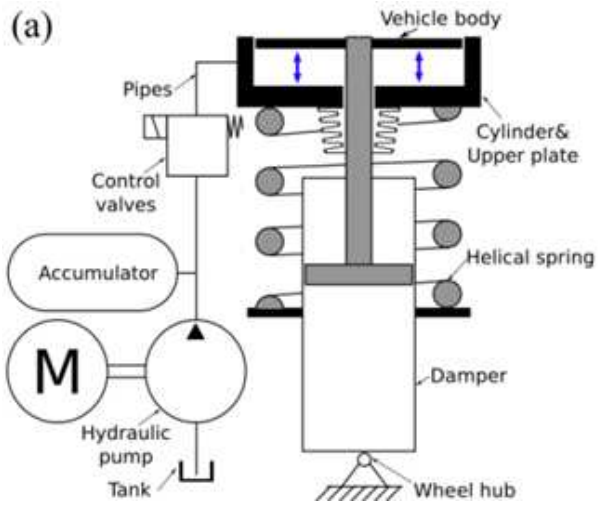

Figure 1.2. Hydraulic schematic suspension system

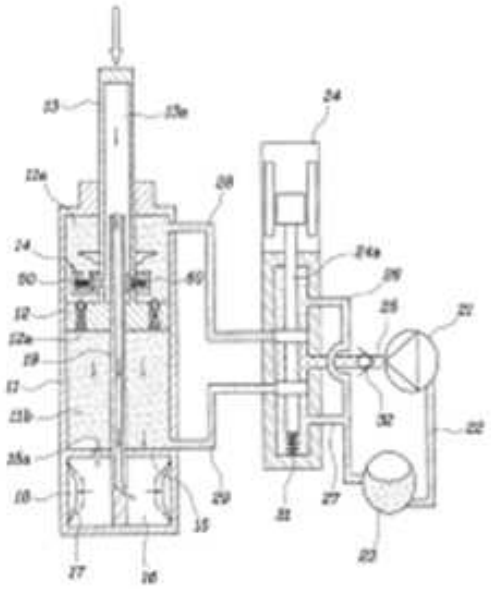

Figure 1.3. Hyundai shock absorber

Also, DaimlerChrysler has patented another active suspension system for vehicles [8] that works similarly to the previous one.

1.3.4 Electromechanical

Starting from the 2000s, new solutions were patented in order to reduce costs and to provide these new systems to the low-cost car segment, however it does not find an application in the automotive field. Most electromechanical height adjustment systems use linear translational parts by a threaded screw-nut mechanism attached to the suspension and an electric motor that can also be connected to a speed reducer [7], shown in figure 1.3.4 (taken from [7]). Audi patented a couple of systems for height adjustment: the first one is composed of a ball-screw attached to an electric motor with a reduction stage of nuts and gear connected to the bottom spring seat [13] (figure 1.3.4, taken from [13]) and the second one, instead, has its own electric motor directly connected to the chassis of the car and the nut connected to the upper plate of the spring [14]. In both cases, the translation of the nut along the axis direction of the shock absorber guarantees the height adjustment.

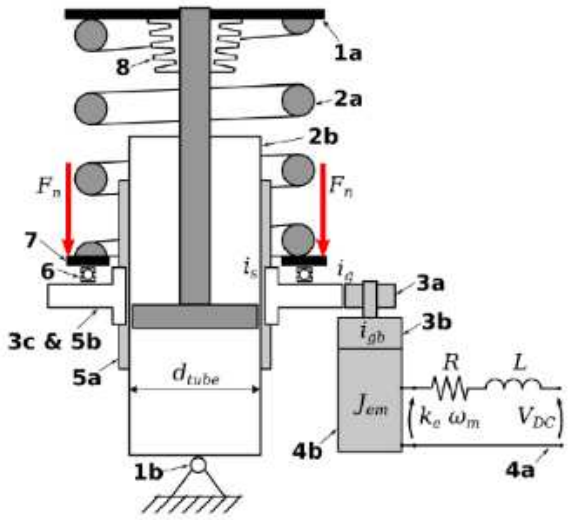

Figure 1.4. Electromechanic system

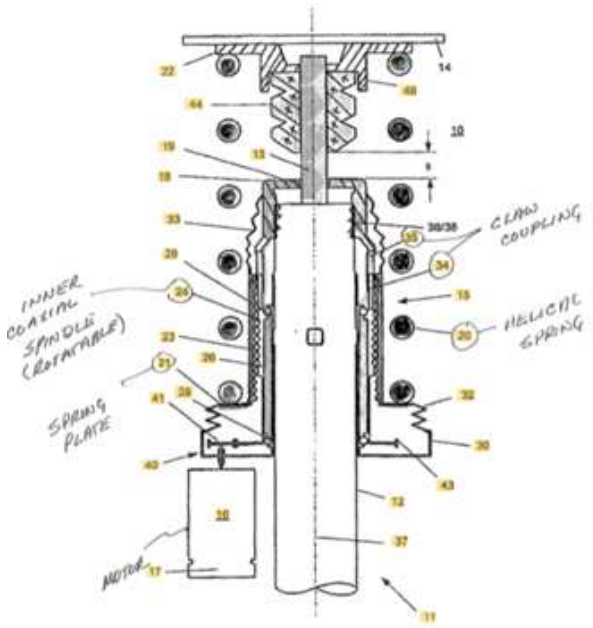

Figure 1.5. Audi height adjustment system

Other non-canonical passive or active height adjustment systems can be described. One easy method to achieve this result is to design a length-adjustable pull rod for a double-wishbone suspension [11]. The assembly of the whole system

consist of only three components: two billets at the end and a coupler, it's composed of two hexagonal bolts end a nut. One of this project's main pros is that the car's height can be easily adjusted without the need to disassemble the entire wheel assembly. The Series Active Variable Geometry Suspension (SAVGS) [1] is a new implementation of the variable geometry active suspension concept that aspires to fill the gap between current semi-active and active solutions, shown in figure 1.3.4 (taken from [1]). Even if it maintains all the elements of a passive or semi-active suspension, in this case, it has introduced a device between one of the end eyes of the spring damper unit and the car's body. The device is mounted in series with a spring-damper system. Once it is actuated, thanks to an electro-mechanic actuator, the position of the end aye changes, modifying the orientation and the elongation of the whole structure. Pros of this system are:

- height control and self-levelling application
- reduces the roll angle and pitch angle
- adjusts load distribution between the axle
- low power consumption

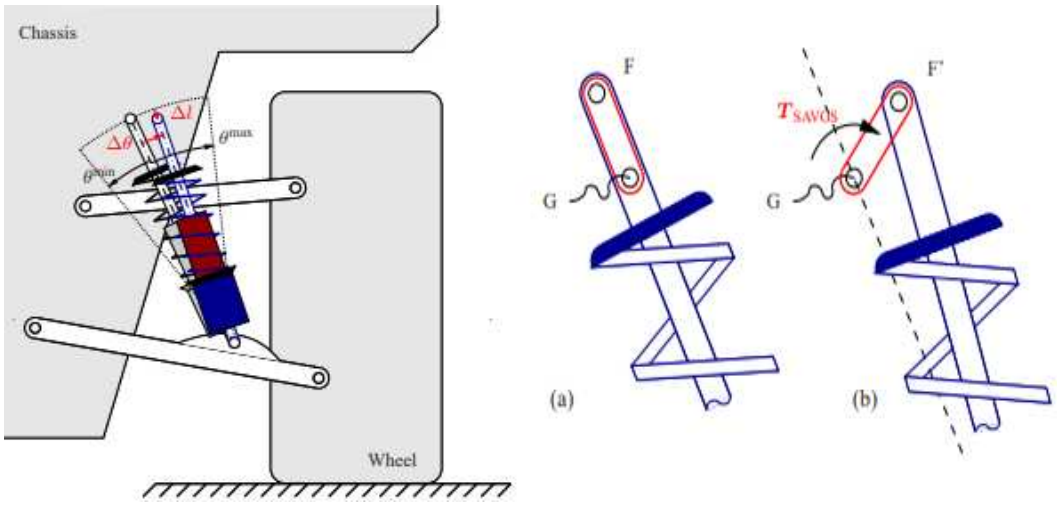

Figure 1.6. SAVGS system

Ford patented in 2018 a particular system of active suspension for its high-performance supercar 2018 GT [3]. This model presents a unique adaptive system that can switch between two modes: comfort and track. The system is a double-wishbone push-road suspension; however, instead of having mounted a single spring,

a torsion bar is connected in series with helical spring and a hydraulic actuator. When the "track mode " is on the actuator compresses completely the helical spring, which in this case behaves as a rigid body. This means that the total stiffness of the suspension system is only given by the torsional bar and the ride height is only 70 mm. When the car is in "comfort mode" the actuator is in minimum encumbrance position, hence the helical spring is free to extend to its maximum stroke and the static ride height is 120mm. In this case the equivalent stiffness of the two springs mounted in series is less than the stiffness of the torsional bar. The system is shown in figure 1.3.4, taken from [3].

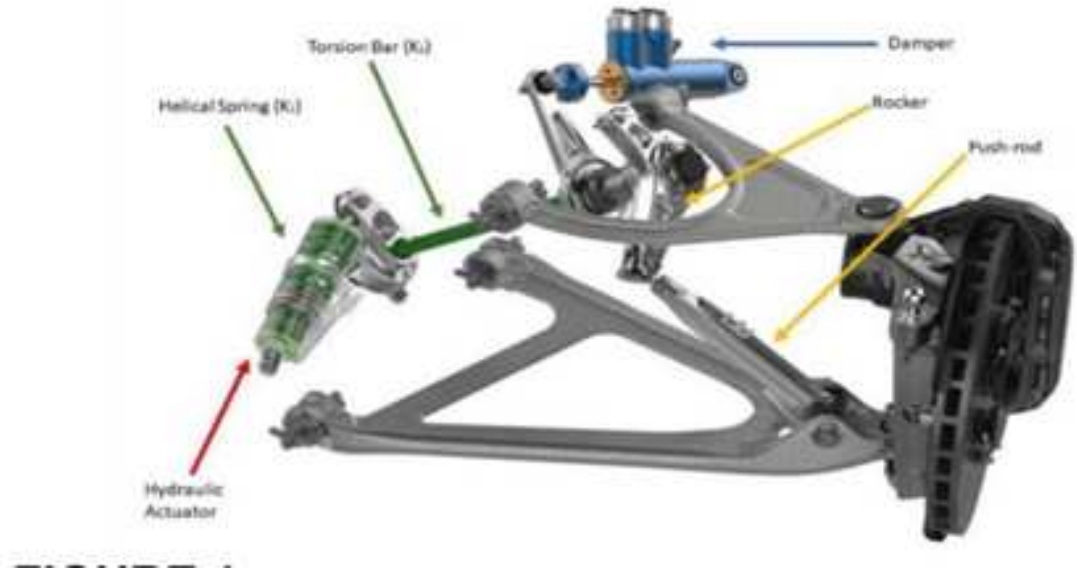

Figure 1.7. Ford GT suspension system

1.4 Anti-roll systems

Body roll is a phenomenon that occurs when a vehicle is approaching a turn. The weight transfer caused by the lateral acceleration during a turn induces the car's roll over its longitudinal axis. Several vehicles make use of a classic anti-roll bar, shown in figure 1.4, that connects the arms of an axle if the wheel suspension scheme is independent, and performs the function of a torsional spring. This bar limits the travel of the two suspensions, preventing them from working simultaneously with excessive compression or elongation. The bar allows transferring, in this case, part of the force of the discharged suspension to the loaded one, resulting in better handling performances. However, if both suspensions undergo the same stress,

the bar doesn't limit the movement, resulting in a better comfort experience. In order to overcome this problem, an anti-roll bar or sway bar is used as one of the suspension's elements that improve the stability or align one wheel against the other. If the spring rate increases in the front, the anti-rollbar will produce an understeer effect, while if the spring rate increases in the rear, it can cause the oversteer effect. Another side effect is that it limits the camber angle change due to body roll but also improves traction [9]. In recent decades, alternating roll control

Figure 1.8. Roll-bar

systems have been developed. An example is provided by the study "PID Controller with Roll Moment Rejection for Pneumatically Actuated Active Roll Control (Arc) Suspension System " [5], in which pneumatic actuators, mounted on each wheel, counteract the roll generated by a lateral acceleration. This system includes a feedback control for managing the heave a roll motion and feed-forward control for managing the load transfer. Other studies provide similar approaches and results to this problem [2]: for example, through an active anti-roll bar (ARC), actuated by an independent electric motor, roll moment is reduced. The control strategy, in this case, is carried out by an LQR controller. These systems have the advantage of being very effective, however they must require a great deal of parameterization based on the type of vehicle, in addition to the possibility of being expensive.

Some researchers have used different approaches, [16] suggests using a hydraulic system capable of controlling pitch and roll without a stabilizer bar. In this case, interconnected hydraulic suspensions are considered, which aim to manage the four

types of wheel-body movements: roll, bounce, pitch and warp.

Mclaren developed an anti-roll system that does not include a solid bar instead, they use a completely hydraulic active system to prevent the car's roll. ''Mclaren proactive chassis control II" can control all the undesired effects due to load transfer of a car. The system presented falls into the category of the interconnected hydraulic suspension system.

The front chambers of the shock absorbers of one side of the car are connected and linked to the rear chamber of the other side. Two small accumulators with a flexible membrane are placed in the hydraulic system; it's possible to regulate the pressure of the gas stored in one side of the accumulator in order to change the damping characteristic of the suspension system. Moreover, in each inlet and outlet port, a flow restrictor is mounted, allowing the control of the stiffness of the suspension system. For example, if the car turns left, the left side shock absorber pistons are compressed, so the front chambers are emptying themselves and, at the same time, are pumping oil into the rear chambers of the shock absorbers on the other side. In this way, it's possible to prevent the roll of the car.

Chapter 2

Workspace description and difference with Simulink approach

2.1 Introduction

In this chapter, it will be explained the simulation toolbox and software used to create and simulate the model of the car's suspension.

To get the best simulation results there are two different paths that are possible to follow: the first one is the canonical Simulink approach, and the second one is to use the Simulink Multibody library. The two approaches may be different in form since the first one is more mathematical while the second one works with a geometrical approach however, the results and the outcomes are the same.

In this thesis project, since there is the need to join two different domains: the mechanical one and the hydraulic one the best choice is to adopt, simulate and model using the Multibody library.

In this chapter will be discussed the reasons behind this choice, the two approaches will be compared, stressing the advantages and disadvantages.

2.2 Simscape Multibody working environment

Simscape multibody is a working simulation toolbox used to simulate mechanical systems like robotic mechanisms, vehicle suspensions and 3D mechanical systems. Thanks to the mechanical joint, constraints, external forces, sensors and geometric bodies which have their own property of mass like inertia matrix, mass distribution and so on. In this way is possible to recreate any mechanical system and study its cinematic and dynamic properties. One of the most important features of this toolbox is the possibility to cooperate with other simscape libraries, this allows to create physical systems in which elements belonging to different domains collaborate, such as in this case, mechanical and hydraulic. Before studying in detail the

models and the used rules, the working environment of Simulink is explained.

2.2.1 Solver configuration

Before discussing the rules of Multibody modelling, it is essential to discuss the configurations used for simulations. The outcome or the success of a test, the quality of the results obtained, and having a direct influence on the simulation timing depends on the choice of the configurator.

First, the choice of the solver determines the strategies used to compute the differential equation of the system. Several options are provided in the "configuration parameters/solver" section. By choosing variable step time several options are provided: ode15s, ode23, ode23s, ode23t, DAESSC. From experience gained using the Multibody, the bests choice are ode15s, ode23t and DAESSC. The ode15s and ode23t solvers can solve index-1 linearly implicit problems with a singular mass matrix $M(t, y)y = f(t, y)$. With DAEs (Differential Algebraic Equation), it is possible to provide the solver's initial conditions for y0 or let, alternatively, then the solver automatically computes consistent initial conditions based on the initial condition you provide for y0. If the provided values are inconsistent, the solver guesses the initial condition automatically, trying to solve the inconsistency.

For the applications studied in this project, the best solver DAESSC, since it solves most of the problems that occur during simulations, such as conflicts and long simulations time.

The variable step size of time steps is chosen since it provides several advantages. Unlike the fixed step size, which solves the model using the same step size from the beginning to the end, the variable udjust the delta time accordingly to the requests of the solver. If a sudden change in the system requires high computation effort, the step size can be reduced or, on the contrary, augmented if the simulation goes smooth. Relative and absolute tolerances can also be tuned to achieve better results, the purpose of these parameters is, respectively, to specify the largest acceptable solver error, relative to the size of each state during each time step and to specify the largest acceptable solver error, as the value of the measured state approaches zero. If the solver error exceeds these values, the step size is reduced.

2.2.2 Library

The following section describes the blocks used for modeling the system. For instance, the workspace, shown in 2.1, contains three fundamental blocks on the left side of the figure:

- Solver configuration: defines the setting of the configurator
- Word frame: provides access to ground or reference frame. This frame is right-handed, orthogonal and unique. The word frame is the ground of all

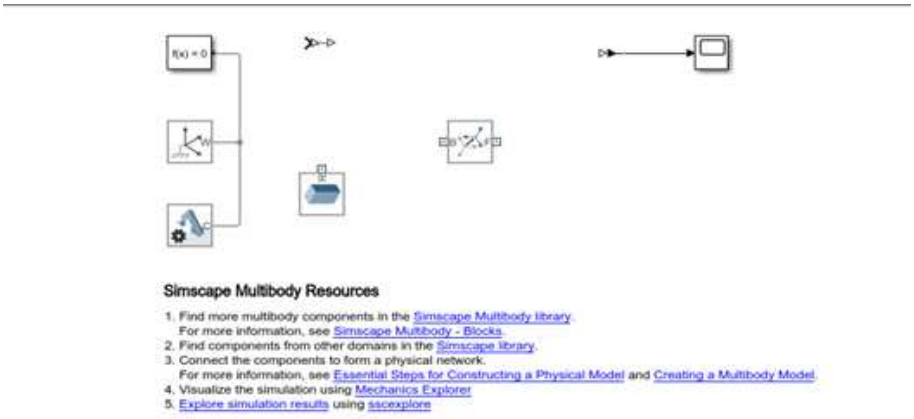

Figure 2.1. Multibody intial workspace .

frame networks in the mechanical model. One model can have several "word frame" blocks but every single one represents the same frame.

- Mechanism configuration: it can define gravity properties for the whole model and also the linearization delta used to compute partial derivatives and linearization.

As mentioned above, the mechanical/physical model require the use of blocks with predefined characteristic. There are several categories of blocks for this reason in this paragraph will be discussed and mentioned only the ones that were used in this project:

- Body elements: this section contains several geometries (cylindrical, solid brick, spherical) and gives the possibility to upload a 3D file from CAD software. Once the geometry is defined the mass properties like the inertia matrix of the solid is automatically computed by imposing the density or the actual mass of the body. One of the most important features consists in the creation of secondary frames on every internal point of the body or on the surface of it. The creation of secondary frames is mandatory since the attachment of two solid bodies takes place through the alignment of two secondary frames

- Frame and transform: since the models are built in a 3D space is crucial to define a Word frame that can be considered as the origin. Secondary frames can be created with the purpose of connecting bodies and joint but, since the modelling of a Multibody system consists of the alignment of frames, it may be necessary to use a "rigid transformations" block. This block allows performing some rigid transformations, like rotation or translation, between a base and a follower frame.

- Forces and torques: These kinds of blocks allow to add internal or external forces and torques to bodies frame, or even "Spring and Damper Force" that, as the name suggests, applies a linear/damped spring force between the two frames that the block is connected to. Custom values of the spring stiffness, damping coefficient and natural length can be chosen. The spring force is attractive between the frames if the spring distance is greater than the spring's natural length.

- Joints: allows the connection of bodies by connecting two frames. There are several typologies of joints: "revolute joint" which allows the body to rotate around the "z" axis of the secondary frame to which is connected, "prismatic joint" which allows a body to move freely along the z-axis, "gimbal joint" which enable the rotation around the three axes x,y,z, "six-degree of freedom" that permits both rotation and translation along the axes and many more.

The elements listed above belong to the Matlab Multibody library of the systems. However, to better understand the correct functioning, other blocks are used, belonging to the canonical Simulink library, such as:

- scopes: useful to visualize signals and parameters

- Math operation blocks which allow performing math operations starting from the signals generated by the blocks.

2.3 Model examples

Once the main blocks are presented it's possible to explain how a model is created.To better understand the modelling rules used in multibody, three examples of mechanical systems are explained, each one with an increasing number of degrees of freedom.

2.3.1 One degree of freedom

The first example is a simple, one-degree-of-freedom system composed of a mass attached to a spring, connected to a reference surface, the scheeme of the system is shown in figure 2.3.1. The mass is free to oscillate under its weight.

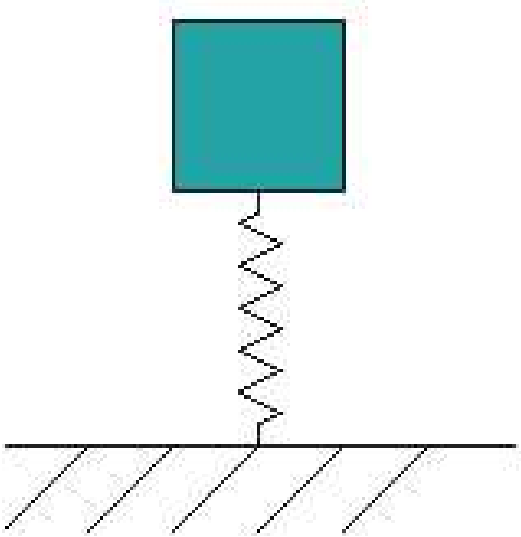

Figure 2.2. One degree of freedom system

In figure 2.3.1 is shown the model realized with the Multibody toolbox. The modelling process starts by creating a reference plane using a "solid brick" block, which has the role of the ground. Two additional secondary frames are created: "origine" is connected to the "world frame" making the two planes united and fixing the reference plane in space, making it immobile. The second one, the "centre" is the secondary plane to which the first end of the spring is attached. As it can be seen, the spring then is connected in parallel to a prismatic joint and in series with the solid brick related to the mass. The joint enables only the mass movement along the vertical axis "z", all the other movements are disabled by the presence of the "prismatic joint" that gives the mass a single degree of freedom. A "rigid transformation block" is added to the system and connected between the reference plane and the ""prismatic joint. In this case, this block provides an offset, equal to the natural length of the spring, between the two secondary frames, otherwise the software builts the two planes at the same point, making the bodies coincident.

Eventually, the scopes are added to visualize all the interesting signals provided by the model's block. In fact, it's possible to sense some characteristics of the systems, for example, position, velocity and acceleration, enabling the sensing features of the joints or, sensing the force of the spring. Figure 2.3.1 shows the visualization window of Multibody in isometric view.

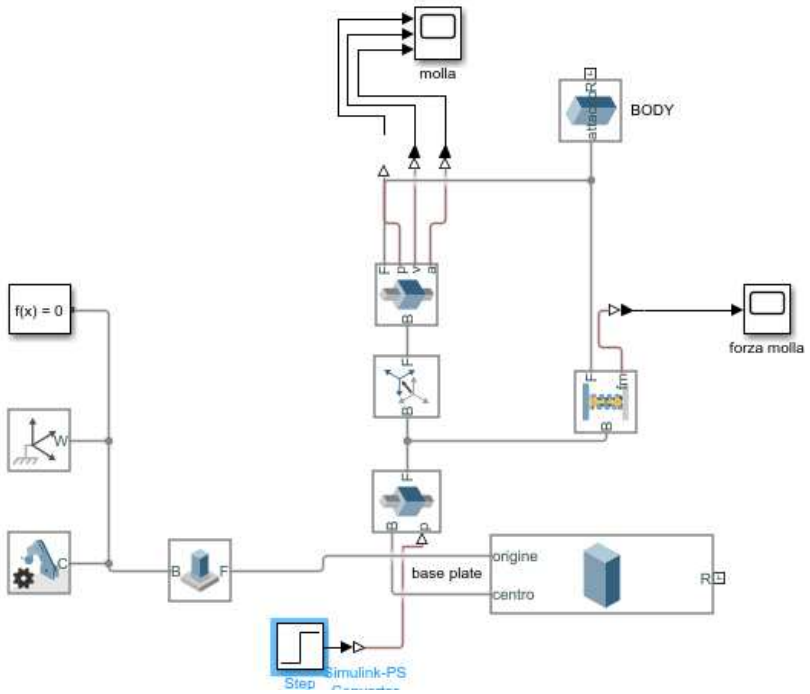

Figure 2.3. One degree of freedom system built with Multibody

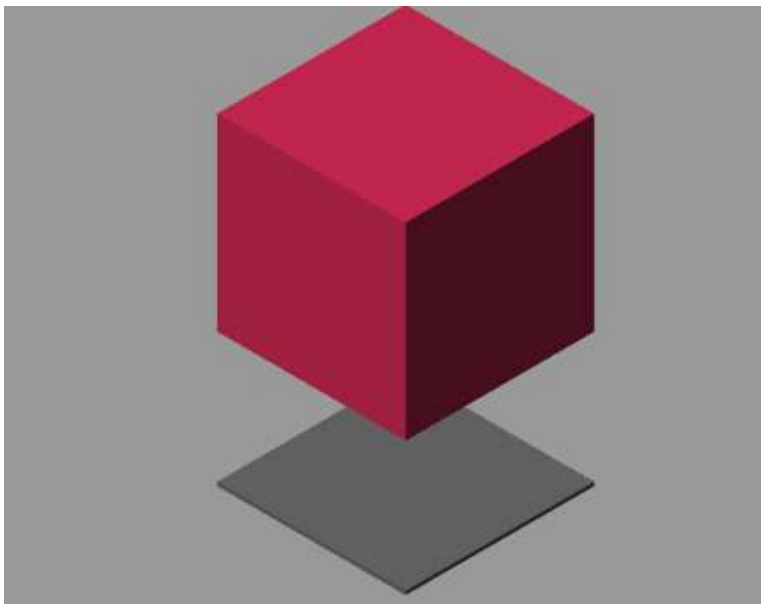

Figure 2.4. One degree of freedom system visualization window

2.3.2 Two degrees of freedom

A two DOF system of a quarter car model is presented 2.3.2. The model is straightforward and it's composed of two masses: m_s represent the car's mass or sprung mass, m_u tyre mass or unsprung mass, K and Kp are the stiffness coefficient of the suspension's spring and tyre, while c represent the damping coefficient of the suspension's shock absorber.
In order to recreate the model using Simulink Multibody, shown in figure 2.6, is crucial to set the Word frame at the base of the reference surface connecting the "world frame" block to the origin secondary frame previously created on the surface of the "solid brick" block. The spring related to the tyre characteristic is then connected to the "central" frame of the reference surface and connected in parallel with a prismatic joint which enables the movent along the z-axis of the word frame and a rigid transformation that translated the unsprung mass by a distance defined in the Matlab script. The spring and the joint are connected then to the R frame which is the frame related to the centre of mass of the unsprung mass. Similarly, the same concept is applied to the sprung mass. In order to avoid problems during the simulation is a good habit to not attach too many branches to the same frame. In fact, as shown in figure 2.6, the solid brick that represents the wheel has two secundary frames but both are placed in the same position: the wheel centre of mass. Two scopes are added to visualize the relative displacement of the springs.

In table 2.3.2 all the coefficients, variables and characteristics of the system are listed: In addition, it's very important to stress the fact that the multibody

TABLE 1	
M_s	475 [Kg]
M_u	70 [Kg]
K_s	80000 [N/m]
K_p	300000 [N/m]
C_s	54772 [N*s/m]

model it's modelled by imposing the geometry of the system, since a time zero, it's crated following the geometrical initial condition given by the "rigid transformation" blocks. However, it's necessary to define some other variables since, otherwise, the system will collapse in one point. To set the correct distance between the reference surface and the unsprung mass and between the sprung and unsprung mass, "rigid transformation" blocks are used, thanks to these blocks the two rigid bodies are shifted by the distances "Rt" and "stroke" along the "z" axis. Once these distances are set it's also important to define the natural length of the two springs, that for simplicity reasons have the same value as the two distances mentioned above.

Table 2.3.2 shows the value of the distance and natural length of the springs:

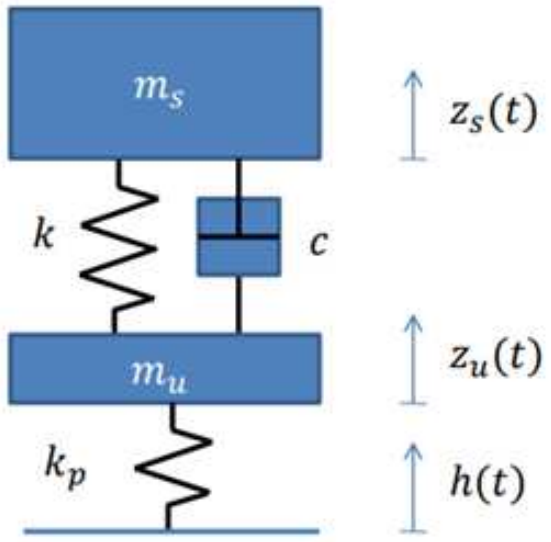

Figure 2.5. Quarter car model, two degrees of freedom

TABLE 2	
L_1	390 [mm]
L_2	600 [mm]
R_t	390 [mm]
$STROKE$	600 [mm]

In this case, L1 and L2 are respectively the natural lengths of the springs mounted between the reference surface and the unsprung mass and the sprung and unsprung mass, while Rt and STROKE are initial offsets related to them.

To simulate the movement of the road's surface another prismatic joint is added between the reference surface and the tyre spring and damper block. The prismatic joint is then actuated with a signal generator.

Once the model is correctly created the simulation starts and all the relevant data, for example, spring displacement, velocity and acceleration of the blocks can be seen through the scopes placed in the Multibody model. Moreover, this toolbox allows us to visualize the physical model behaviour during the simulation time which is very important for several reasons: helps to confirm that the model is created correctly with the expectations and allows the user to visualize the static and dynamic behaviour of the physical system under the influence of different inputs. Figure 2.10 shows the visualization window and the model displayed in it. As is shown in the figure the two solid brick blocks related to the sprung and unsprung

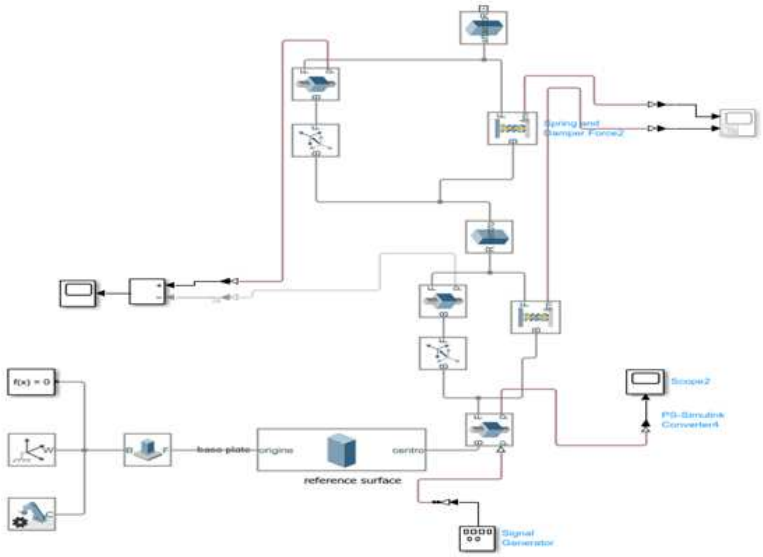

Figure 2.6. Quarter car Multibody model

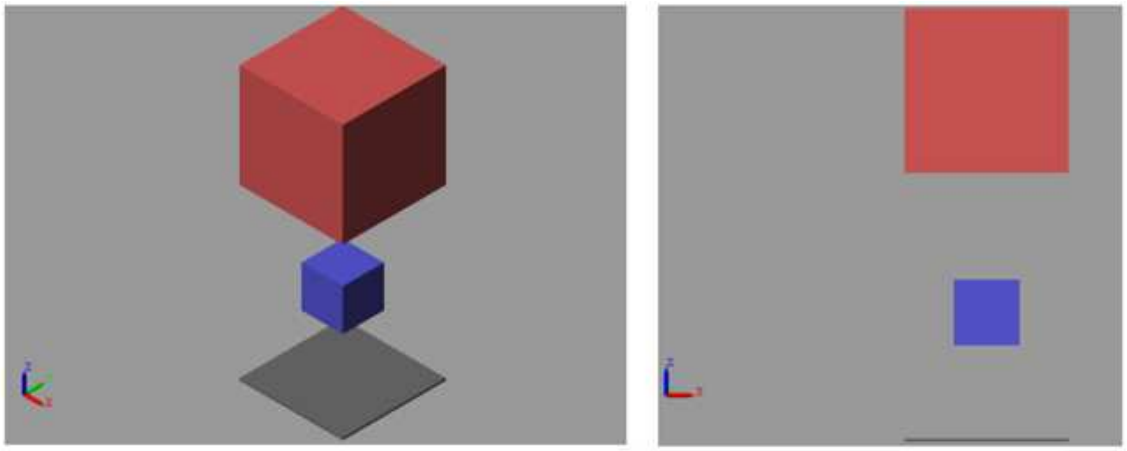

Figure 2.7. Visualization window: isometric and frontal view

mass and the reference surface are clearly visible while the spring placed between them is not. In fact, Multibody permits only the visualization of the body blocks.

2.3.3 Five degrees of freedom

The last example provided is a five degrees of freedom system that represents a car's axle. It is composed of two unsprung masses and a sprung mass. The modelling procedure is the same of the previous case, the only particularity is given by the system's constraint. Analyzing figure 2.3.3, it can be noticed that:

- the sprung mass can rotate around the y-axis and along the z-axis, so it has 2 degrees of freedom.
- Left unsprung mass has one degree of freedom since it can only move along the z-axis
- Right unsprung mass has 2 degrees of freedom since it can slide along the x and z axes.

The reason behind this configuration is that when the body' vehicle rolls, it causes a translation of one of the two unsprung mass along the x-axis. If both are hinged to the ground, the system is hyperstatic, which means that the number of constraints is bigger than the degrees of freedom of the system and the simulation's software is unable to compute the internal forces and reactions of the structure.

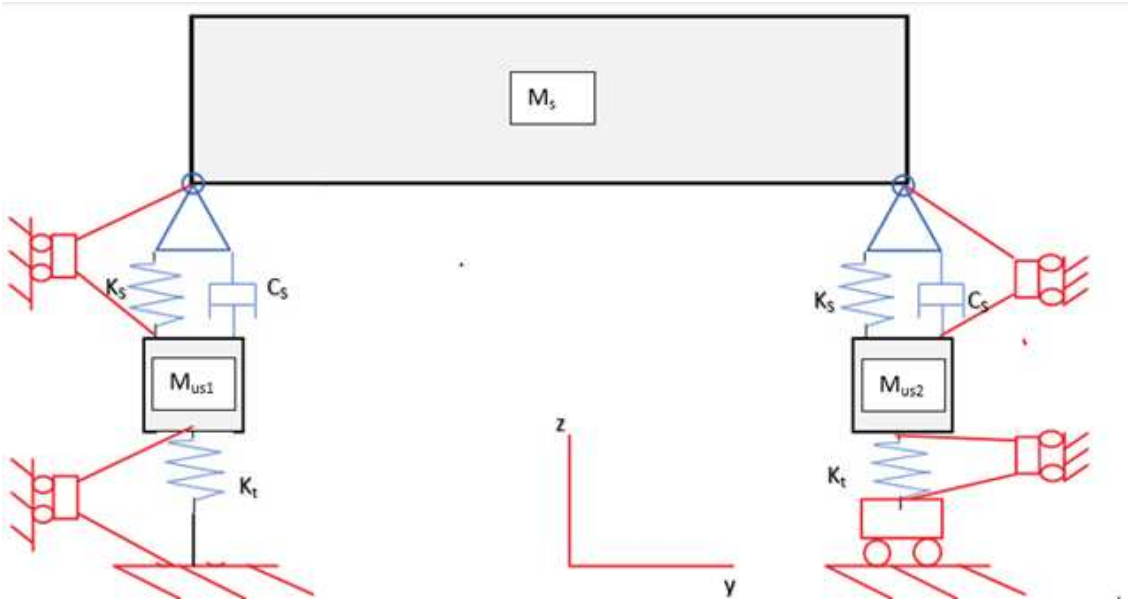

Figure 2.8. Car's axle scheme

The modelling process is similar to the 2 degrees of freedom system. First is created the reference plane, then two secondary frames are generated on the upper

surface of the reference plane. These two frames, one on the right and one on the left, will be the references to which the unsprung masses of the vehicle will be connected.Similarly, two other secondary frames will be created on the lower surface of the car body, one on the right and one on the left and are the attachments for the vehicle suspension springs. The modelling procedure is the same proposed in the previous section, the springs related to the tire characteristic and the suspension are always mounted in parallel with a "prismatic joint" allowing the vertical movement of the sprung mass and unsprung mass. In this case, the roll behaviour is achieved by connecting two "revolute joints" between the upper end of the spring and the lateral frames of the car. Since the "revolute joint" allows the rotation only around the z-axis of the frame to which it is attached, two "rigid transformation" blocks are connected before and after the joint. The aim of these blocks is to apply a frame rotation to the lateral car frame in order to align the axis with the revolute joint.

The same consideration is applied to the right side of the car, however, an additional prismatic joint is placed between the right frame of the reference plane and the spring base frame. Also in this case, two additional "rigid transformation" blocks are placed before and after the prismatic joint, since the translation of this component happens only along the z-axis. These two blocks perform a rotational transformation allowing the perfect alignment of the frames.

The Multibody model and the visualization window are displayed in figure 2.3.3 and 2.3.3

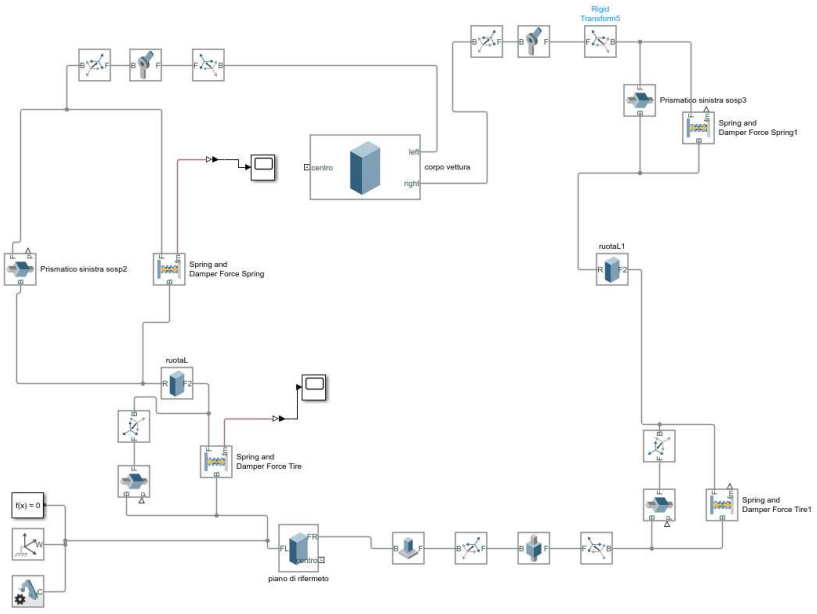

Figure 2.9. Multibody car axle model

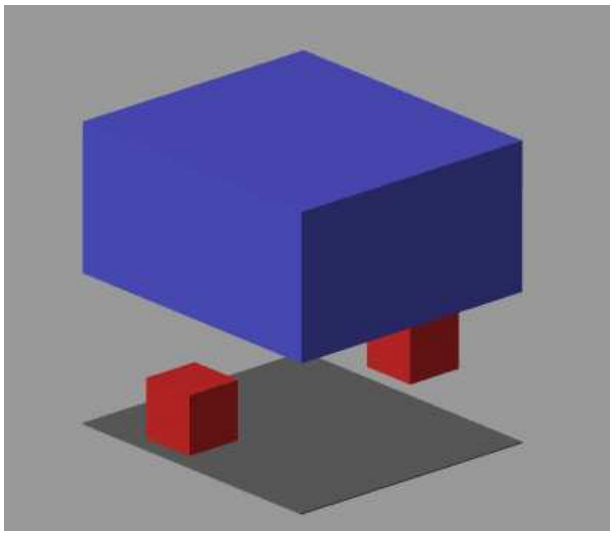

Figure 2.10. Car's axle visualization window

2.4 Differences between mathematical and geometric approaches

In this section will be compared the modelling differences between the two approaches: mathematical (Simulink) and geometrical (Multibody). In this case, the two degrees of freedom quarter car model, presented in section 2.2 is taken as an example since is a good compromise between complexity and manageability.

2.4.1 Multibody

As mentioned in the previous section, where is described the creation procedure of the considered model, it's important to add some other considerations: there is no need to compute or derive the equation of motion of the system since, once the model is generated by the multibody toolbox, the equations are automatically derived by the toolbox. For this reason, is crucial to use the correct blocks that respect the wanted geometry and define constraints and degree of freedom of each body element.

For example, in this case we have two degrees of freedom system composed of two masses which cannot rotate around any principal direction and can only slide along the "z" axis. As shown in figure 2.6, this task is obtained by placing between the ground and the un-sprung mass and between the two masses two prismatic joints. In this way, the two bodies can only move along the vertical direction because

the prismatic joints remove the three rotational and two translational degrees of freedom.

2.4.2 Simulink

This method, unlike the other, requires computing manually the equation of motion of the system, starting from the sketch of the model and then writing these equations in the Simulink ambient.

Also in this case it will be considered the quarter car model presented in figure 2:

$$\begin{cases} m_s\ddot{z_s} = -c(z_{s-\dot{z_u}})-k(z_s-z_u) \\ m_s\ddot{z_s}s = -c(\dot{z_s}-\dot{z_u})-k(z_s-z_u)-k_p(z_u-h) \end{cases} \tag{2.1}$$

These equations can be expressed in matrix form:

$$[M]\ddot{q}+[C]\dot{q}+[K]q=[H]h \tag{2.2}$$

Where the varius contributions are:

$$q=\begin{bmatrix} z_s \\ z_u \end{bmatrix}[M]=\begin{bmatrix} M_s & 0 \\ 0 & M_u \end{bmatrix};[K]=\begin{bmatrix} k & -k \\ -k & k_p+k \end{bmatrix};[C]=\begin{bmatrix} c & -c \\ -c & c \end{bmatrix};[H]=\begin{bmatrix} 0 \\ k_p \end{bmatrix}; \tag{2.3}$$

Once the equations are written in matrix form, to be computed and simulated, these are written in Simulink workspace using the commonly used and math blocks. Isolating the terms with the largest order of differentiation it becomes:

$$\ddot{q}=[M]^{-}1(-[C]\dot{q}-[K]q+[H]h) \tag{2.4}$$

In figure 2.11, the created model is shown:

2.5 Results comparison

In this section, it will be discussed and compared the results given by the two methods in different conditions. Even if the two approaches are substantially different in form, they give back the same results

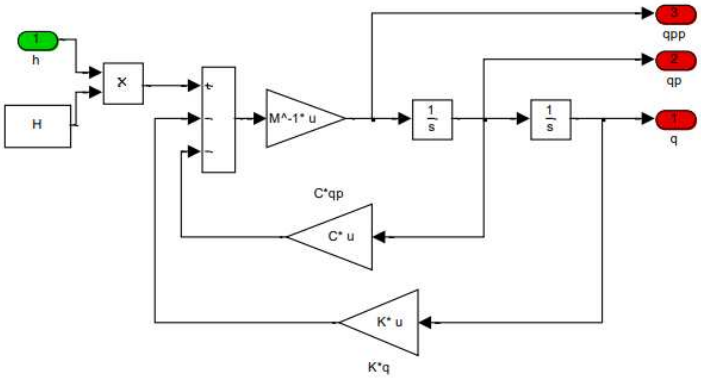

Figure 2.11. Simulink model

2.5.1 Free response

In order to make the results comparable between them, it's necessary to slightly modify the previous Two-degrees of freedom Multibody model. The reason for this change is due to the fact that the mathematical/Simulink approach has an equilibrium condition equal to zero, this means that when is not given any input to the system the two masses are still. This system does not take count of any offset or the natural length of the spring since it's not relevant while studying the response of the system to external input. In Multibody the equilibrium condition necessary to study the vibrational response of the system can be obtained in two ways: the first one consists of adding a spring preload equal to the weight force of the mass acting on the spring, the second one, instead, is to properly compute the initial position of the body knowing its weight, the stiffness of the spring and its natural length. Knowing all these characteristics is possible to compute the compression or the elongation of the spring and then set the initial condition to obtain no oscillation. However, this second method it's more complicated as it is subject to computational errors.

In figure 2.12 is shown how this result is obtained, adding in parallel to the two springs the internal force block.

the next figure 2.13 it's possible to compare the two results obtained with and without the spring's preload: in the first case, the system tends to fall under its weight, in the second case this phenomenon it's compensated by the applied preload and the position it's perfectly set to zero.

The next susbections will compare the results of the two methods given an external input. Since the system taken as example is a quarter car model it's important to study its behaviour while the road profile is changing. All the characteristics of the system, once again, are expressed in table 1 Two cases will be analysed:

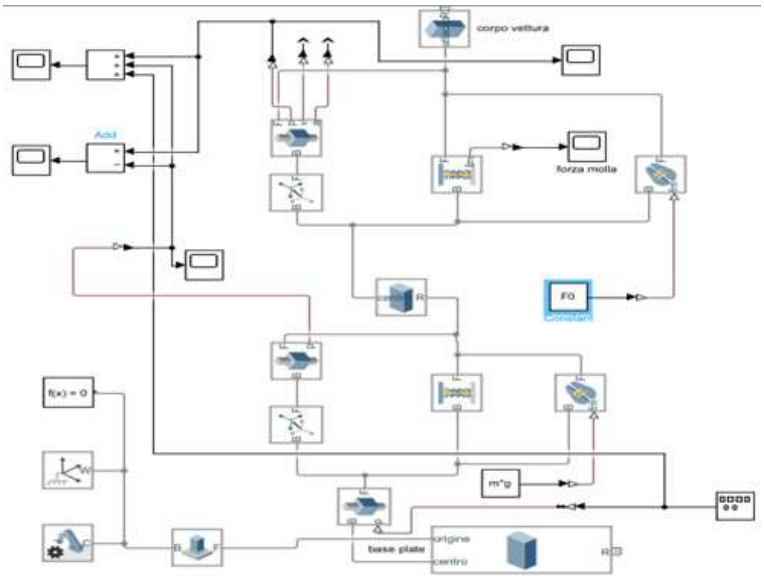

Figure 2.12. Multibody model with spring preload

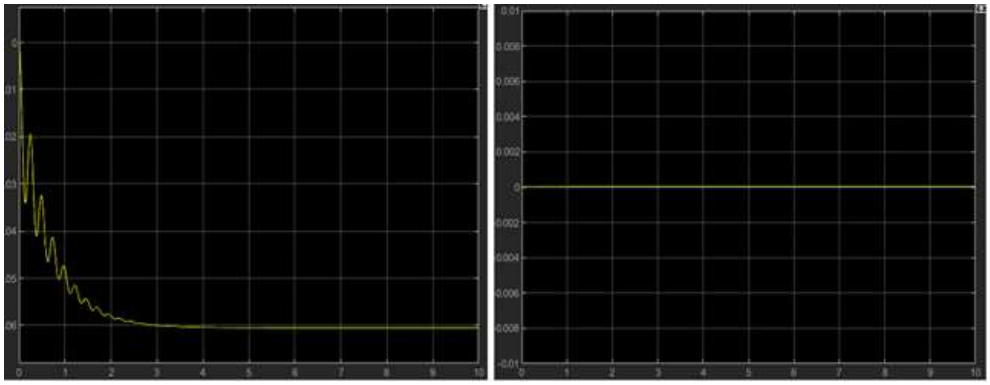

Figure 2.13. position without and with spring preloads

sinusoidal input and step input.

2.5.2 Sinusoidal input

In this case, the objective is to study how the two methods react to a sinusoidal input of amplitude A=0.01 m and a frequency of 0.4 Hz.

As it can be noticed from figure 2.14 the relative displacement of the two bodies respects their original position, which by the way is the equilibrium static condition,

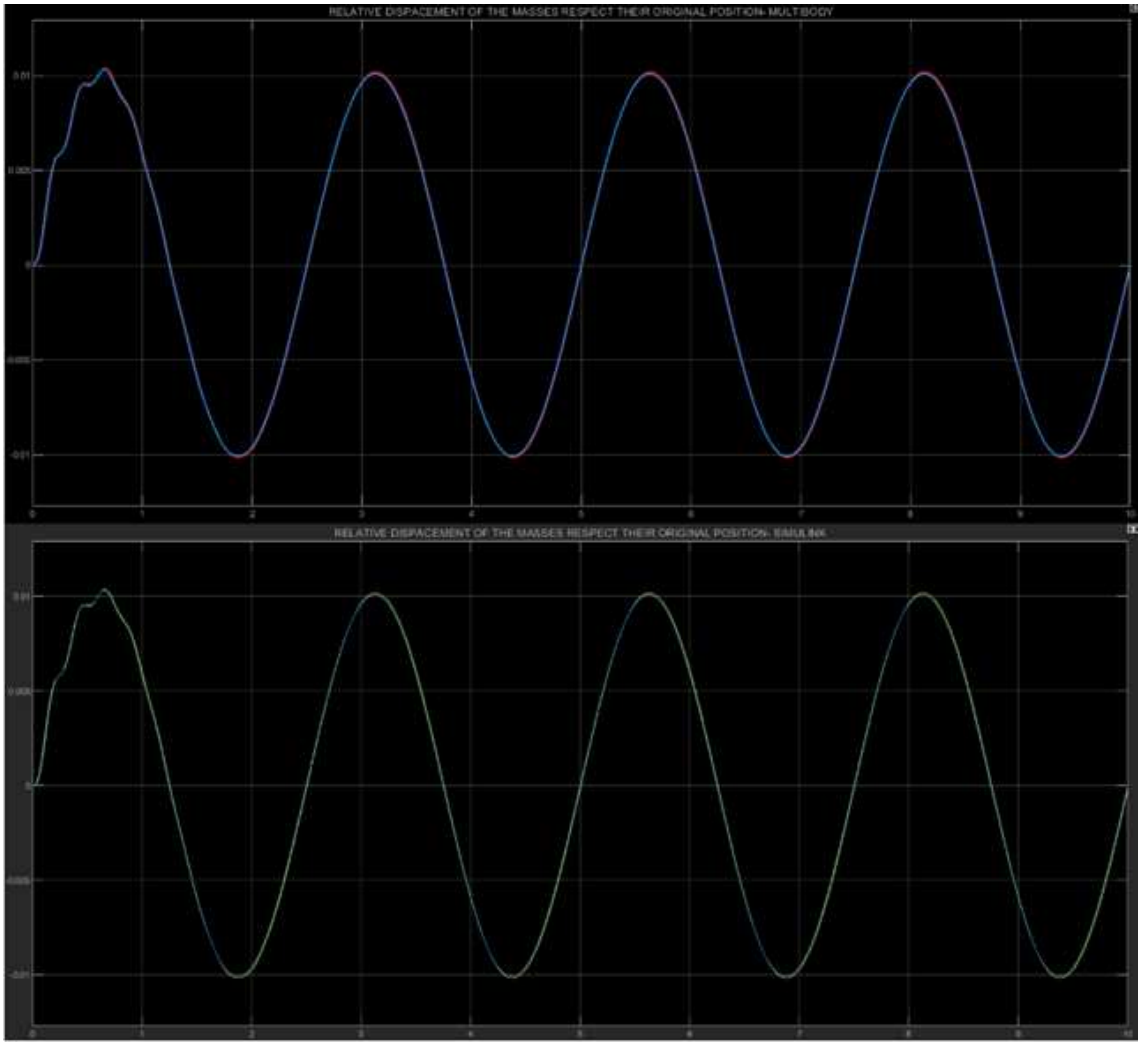

Figure 2.14. Relative displacement

are perfectly equal. In each subplot are present two different lines related to the masses.

To prove the consistency of the two solutions the suspension spring displacement is compared. As it's possible to observe from figure 2.15 the performances are the same, however a small offset is present in the multibody system. This offset is probably due to the computational process of the software, but since the magnitude is in the order of a few tenth of micrometre it's negligible.

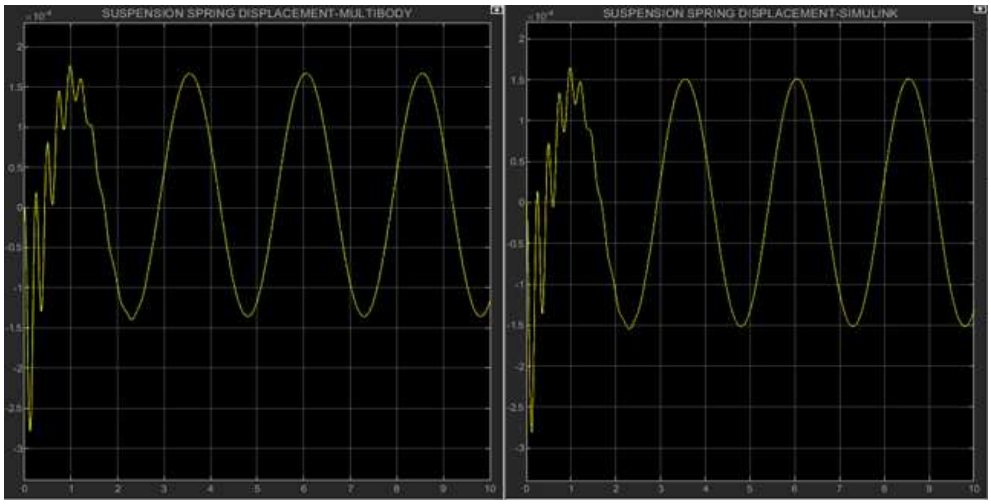

Figure 2.15. Suspension spring displacement

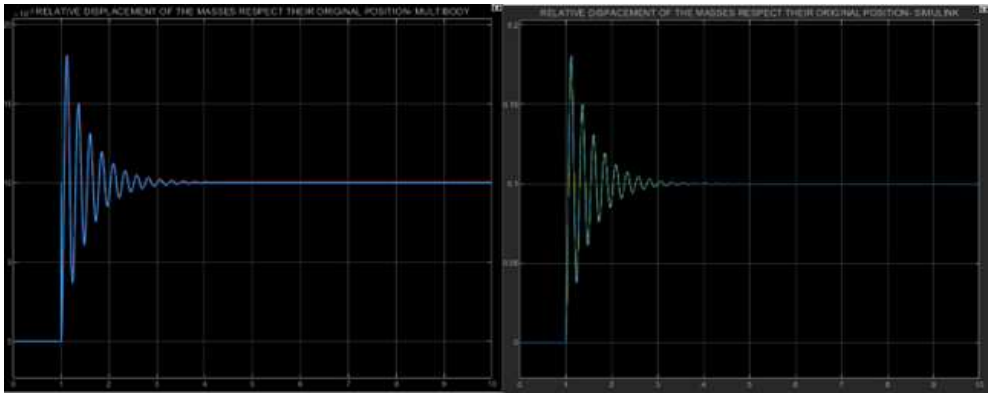

Figure 2.16. Relative displacement

2.5.3 Step input

In this test a step signal is applied to the system, the behaviour of the two approaches also in this case is similar. As shown previously, it will be compared the results of the relative displacement (figure 2.16) and the suspension spring displacement (figure 2.17)

As mentioned above, also in this situation it's possible to notice a small offset in the Multibody model result, however since it's very small it can be neglected.

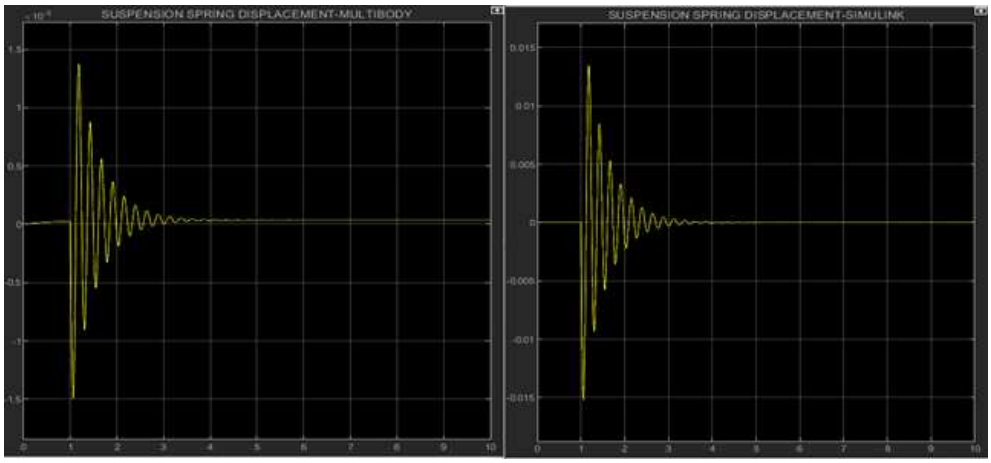

Figure 2.17. Suspension spring displacement

2.6 Final Considerations

The results that emerge from the two simulations' procedures are very similar. Although Multibody may suffer from errors in the modelling phase that may lead to small some unexpected behaviour, like the offset already discussed, and the difficulties that can emerge during the construction of the model it's the toolbox chosen to study the physical systems.

The reasons behind this choice it's attributable to the fact that the mathematical/Simulink approach gives good results whit small or simple physical systems, but considering that the goal it's to study an active car suspension system with integrate hydraulic components, the best choice is to complete the research with this toolbox. In fact one of the most important features is the compatibility with Simscape library, which allows to develop a model linking together the mechanical system with the hydraulic one.

Chapter 3

Model description

In this chapter will be discussed the methodologies and the construction rules used to build the model. Starting from the scheme of the geometry of the model, taken from a CAD file, it's possible to determine all the size of the components. It's important to underline that the presented model is a two dimensions approximation of the real geometry of the rear axle of the car.The entire model is presented in figure 3.The model here presented has 8 degrees of freedom, analysed in detail:

- **Body**: the car's body has three degrees of freedom, two translational along the z and x axis and one rotational around y-axis
- **Right wheel**: two degrees of freedom in total, one tranlational (z-axis)and one rotational (y axis)
- **Left wheel**: unlike the right wheel, this one has, in addition, a translational degree of freedom, so in total it has three DOF. The reason behind this choice is that if the car stat to roll, the additional degree of freedom applied to the wheel allows it to slide otherwise, the system results in hyperstatic condition and the solver is unable to perform the simulation.

Table 1, shows only information that the company is willing to share, the size of the components such as weight of the car, the position of the suspension links and the wheel's hub are not listed for privacy reasons. The obtained scheme is the following indicated in figure 3.1:

TABLE 1			
COM height	h	0,722	m
Track	t	1,820	m
Sprung mass	M_s	1000	kg
Unsprung mass	M_{us}	70	kg

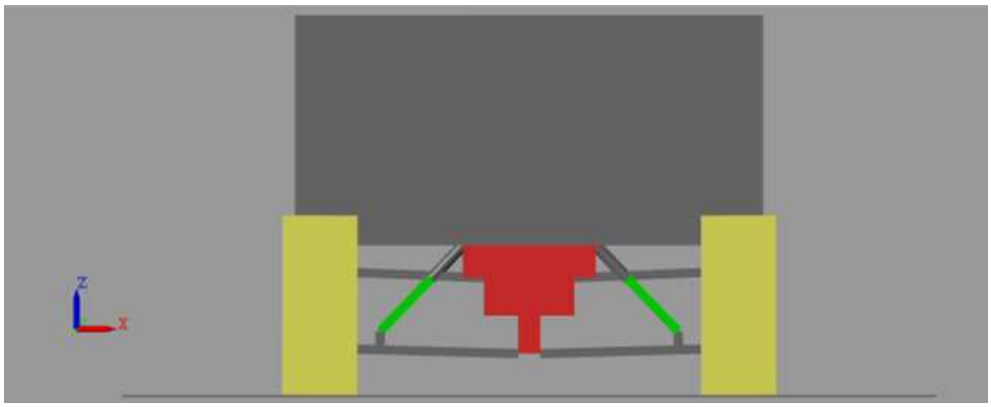

Figure 3.1. Rear axle Multibody model

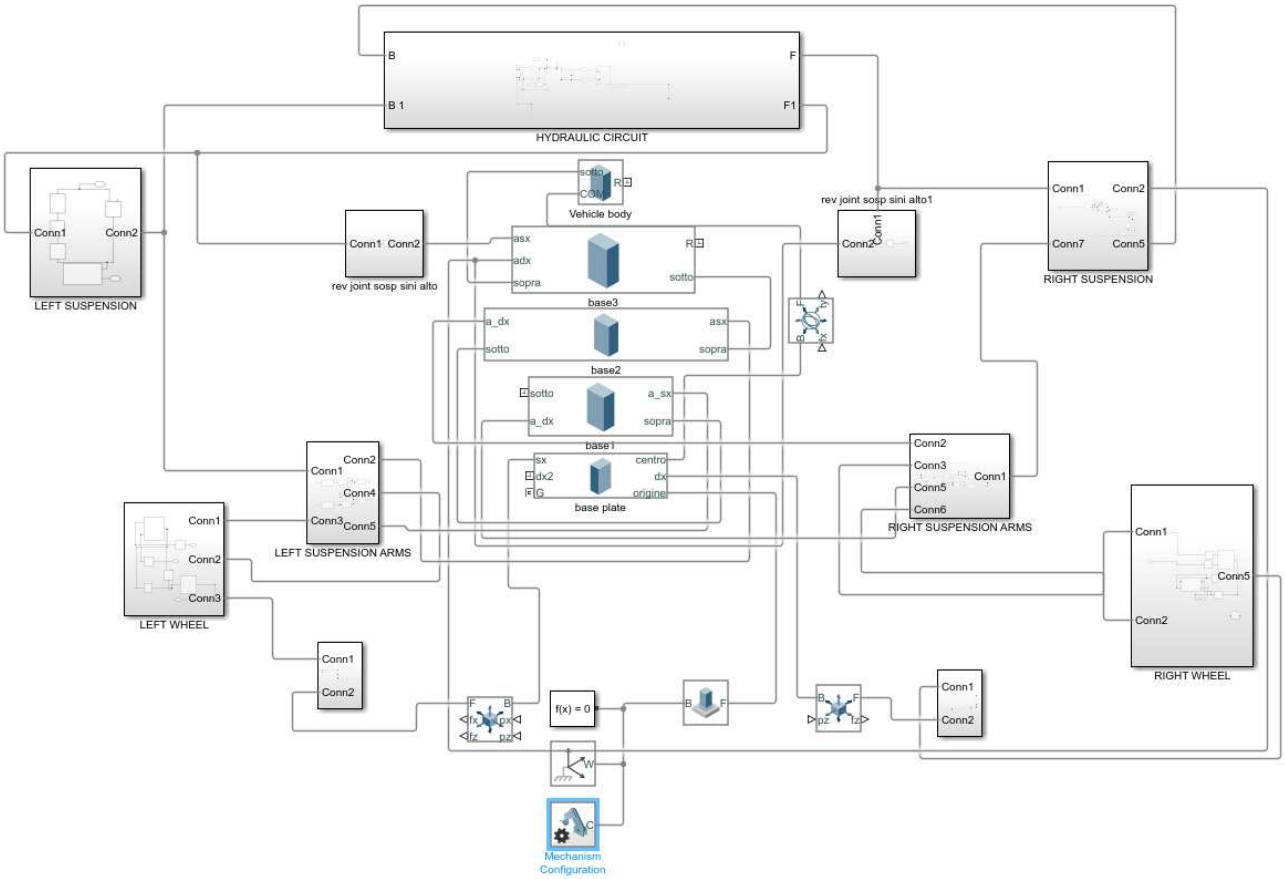

Figure 3.2. Multibody model

To describe the system in a proper way the description is divided in several subsection, each one describe a different part of the model.

3.1 Car's body

The starting point of the modelling process starts by creating the body of the car, which is composed of four different solid bricks. The linkage between the bodies is done by connecting the secondary reference frame previously created. The positioning of these secondary frames is such as to allow the main axes, passing through the centre of gravity of each block to be aligned with each other, allowing a perfectly symmetrical configuration. Another important feature is the linkage between the main block and the "base plate" performed by a "six-degrees of freedom" block which allows the translation and rotation along the 3 axes, although the model is meant to rotate only around the y-axis and translate along lateral and vertical directions.

The six degrees of freedom joint is chosen also for other important aspects, gives more stability to the system during simulation, avoiding warnings and moreover allows to apply several inputs to the car's body.

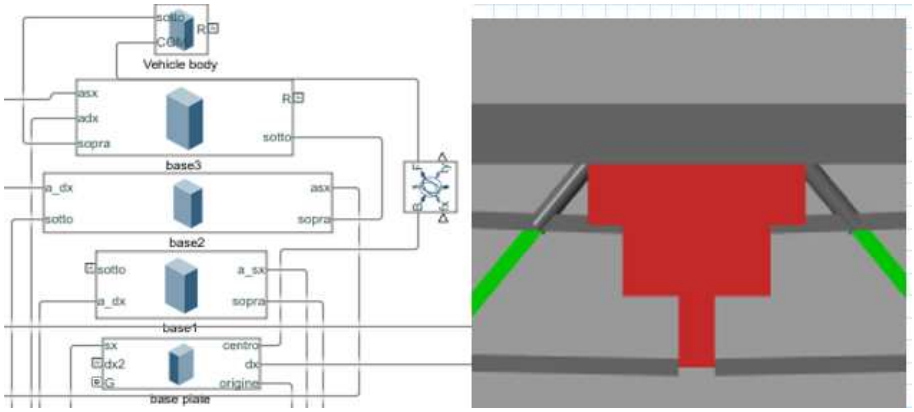

Figure 3.3. Body connection scheme using Multibody blocks

3.2 Suspension scheme

For simplicity, it is considered only one side of the vehicle since, for symmetry reasons, it is redundant to describe both sides of the rear axle. The studied system is a double-wishbone suspension, characterized by two oscillating and overlapping triangular arms, the lower and upper ones, forming a quadrilateral. One of the pros of the double-wishbone configuration is that by changing the length and arrangement of the arms, it is possible to vary the roll centre as desired, allowing

to steer the wheel with absolute precision and have reasonable control over the wheel's camber angle. Once the main body is modelled, the next step is to create the suspension's arms, as shown in the figure 3.1, the entire suspension system is made two-dimensional consequently, the arms are modelled as parallelepipeds using "solid brick" blocks. First, it is important to underline that the subsection illustrated contains the joints which enable the solid bricks to move and rotate. Since the arms are supposed to rotate only along the y-axis, the revolute joints are connected to "rigid transformation" blocks that aim to align the joint's frames with the solid brick frames.

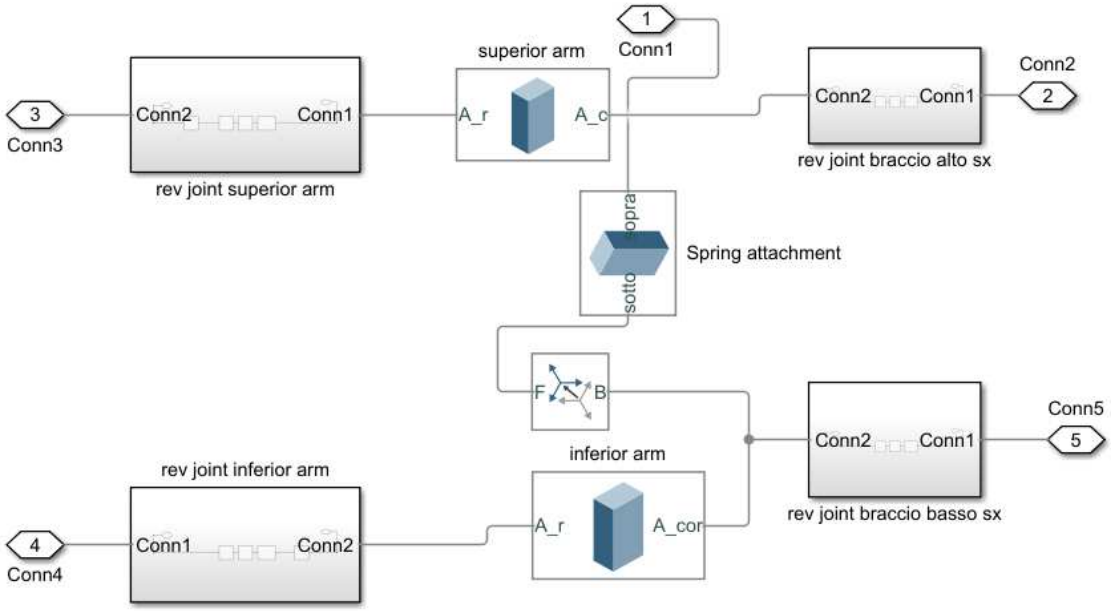

Figure 3.4. Arms connection scheme using Multibody blocks

The inferior arm is attached to Base 1 (see section 3.1) through connection 5 and to the wheel thanks to connection 4; similarly, the superior arm is connected to the body and the wheel, respectively, through connections 2 and 3. Eventually, the spring attachment is created using a "brick solid block", connected to the lower arm body connection frame and shifted of a given value, thanks to the proprieties of the "rigid transformation block". The last cited block has the function of anchor point for both spring and hydraulic actuator (connection 1). The connection scheme is illustrated in figure 3.2 It is crucial to underline that all the blocks are massless since the real component characteristic are unknown. In fact, the sprung mass is only considered at the wheel.

A second subsystem completes the suspension unit, which contains the characteristic spring mounted in parallel with the hydraulic cylinder. The subsistem

shown in figure 3.2, as already mentioned above, contains the "rigid transformation" Blocks and the revolute joint necessary to perform the correct movement to the suspensions. From the observation of the scheme, it can be noticed that the spring is mounted in parallel with two solid brick blocks, whose function is to display the relative displacement of the spring during the simulation. As already mentioned, the springs are not visible in the visualization window; therefore, these two blocks are added to check the correct functioning of the model. The prismatic joint linked between them is meant to enable only the translation along their z-axis. The spring is attached, instead, to Base 3 thanks to connection 1.

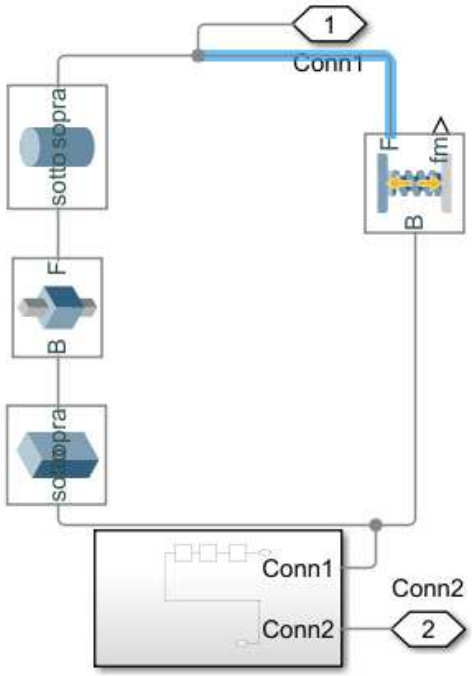

Figure 3.5. Spring connection scheme using Multibody blocks

3.3 Wheel scheme

It is one of the most important parts to consider during modeling, since it considers the tire's deformation subject to the weight force of the car and the load transfers when cornering. To achieve this goal, the wheel compartment is divided into two sections: the tire and the unsprung mass. The tire block is massless and in contact with the ground. The wheel compartment is divided into two sections: the tire and the unsprung mass. The tire block is massless and in contact with the ground.

The tire is connected to the ground thanks to connection 3, from the secundary reference frame placed at the bottom of "Tire solid brick" the spring related to the elastic characteristic of the wheel is attached. The spring is then connected in parallel with a prismatic joint and then connected to the centre of mass frame related to the unsprung mass. The spring stiffness is set to a value defined in the Matlab script and is equal to $K_t = 300K\frac{N}{m}$. To end up, the unsprung mass is connected to the arms of the suspension thanks to connections 1 and 2. However, as it is possible to observe, two rigid transformation blocks are added with the aim of sliding the attachment point of the arms. The presented configuration allows recreating the behaviour of a deformable wheel.

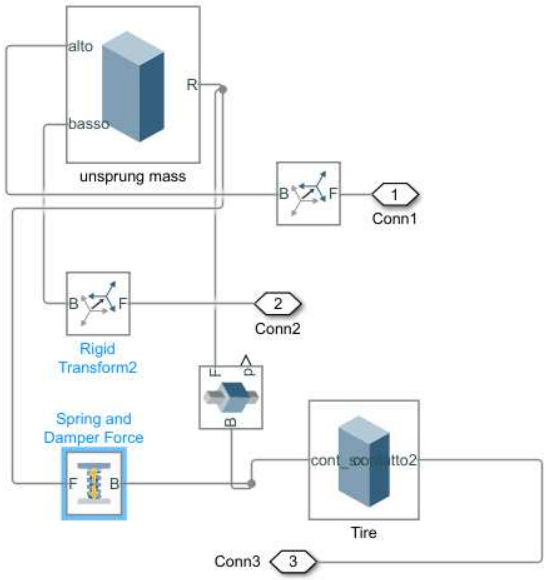

Figure 3.6. Wheel connection scheme using Multibody blocks

3.4 Hydraulic circuit

As mentioned in chapter one, an alternative to the passive anti-roll bar device is represented by a hydraulic system composed of two hydraulic cylinders, which substitute the classic anti-roll bar system. Each cylinder is connected to the other one using two hydraulic connections: the upper chamber of an actuator is linked to the bottom chamber of the other actuator and vice versa. In addition, are added two gas chamber accumulators and four flow restrictors, each one is placed at the outlet port of the hydraulic cylinder. Each cylinder is then connected in parallel to the suspension's spring. The complete scheme is shown in figure 3.4.

The working principle is simple, for example, the car is turning left, in this case, the right suspension is compressed so the fluid inside the upper chamber of the actuator is pushed through the hydraulic circuit to the bottom chamber of the left cylinder. The increasing pressure pushes the left piston up and, as a result, there is a noticeable reduction in the car's roll angle.

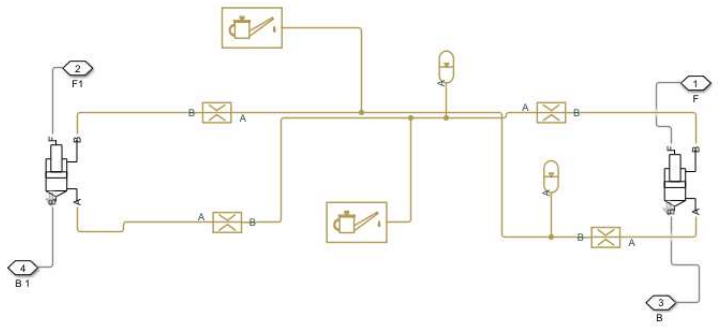

Figure 3.7. Hydraulic circuit scheme

The hydraulic components, illustated in figure 3.4, are explained below.

- **Hydraulic cylinder**: high tunable element. In particular, its modelization considers the internal friction forces, hardstop and compressibility, however, the only parameter considered and tuned are the ones related to the dimension of the actuator, such as: stroke and areas of upper and lower chambers
- **Gas charged accumulator**: The accumulator consists of a precharged gas chamber and a fluid chamber, separated by a diaphragm, the fluid chamber is connected to a hydraulic circuit. When the fluid pressure inside the accumulator becomes greater than the precharge pressure, fluid enters the accumulator and compresses the gas. A fluid pressure decrease causes the gas to decompress and discharge stored fluid into the system. The separator motion is restricted by a hard stop when the fluid volume is zero and when the fluid volume is at the fluid chamber capacity. The fluid chamber capacity is the total accumulator volume minus the minimum gas volume. The componet presented is crucial for the dynamic of the system. It has several parameters that can be modified in order to achieve the best results, such as the Precharged pressure of the accumulator (P), the volume of liquid at time zero inside the components (Vliq), the specific heat ratio (K), the hard stop damping and stiffness coefficient and the minimum volume of gas inside the chamber. The equation characteristic of the accumulator is :

$$(P_g + P_a)(V_t - V_f)^k = (P_p r + P_a)V_t^k \tag{3.1}$$

Where P_a is the atmospheric pressure, P_g is the gas pressure, V_t and V_f are the total and fluid volume into the chamber and P_{pr} is the precharged pressure.

- **Local resistance**: the local resistance block creates a generic resistance into the hydraulic circuit, for example, a change in the flow section. The pressure drop is linked to the K coefficient in the model parametrization, which is the pressure loss coefficient listed in tables, textbooks or catalogues. The following relation gives pressure drop:

$$\Delta P = P_A - P_B \tag{3.2}$$

P_A and P_B are the pressures computed at port A or B. The relations that relates pressur drop with flow rate is:

$$q = A\sqrt{\frac{2}{K\rho}}\frac{\Delta P}{(\Delta P^2 + P_{cr}^2)^{\frac{1}{4}}} \tag{3.3}$$

As already mentioned, the "K" is the pressure loss coefficient and it is constant, A is the section area of the local resistance, ρ is the fluid density and P_{cr} is the minimum pressure for turbulent flow.

- **Hydraulic fluid**: The block presented is used to assign the fluid characteristic, it has to be connected to each branch of the circuit to be effective otherwise the system behaves in an uneffective way. It is possible to choose between several typologies of fluids, in this way the characteristic such as, density and viscosity are automatically determined. In this case the chosen fluid is transmission fluid AFT(dexron III).

Chapter 4

Kinematic study of the suspension system

In this section we will discuss the kinematic nature of the modeled suspension.

The data characterizing the kinematic component of the suspension were extracted from the CAD file under examination, containing the geometry of the illustrated suspension.in this project thesis will be analized only the suspension scheme of the rear axle of the car, which, in figure 4.1, the specific characteristics of the geometry are explained:

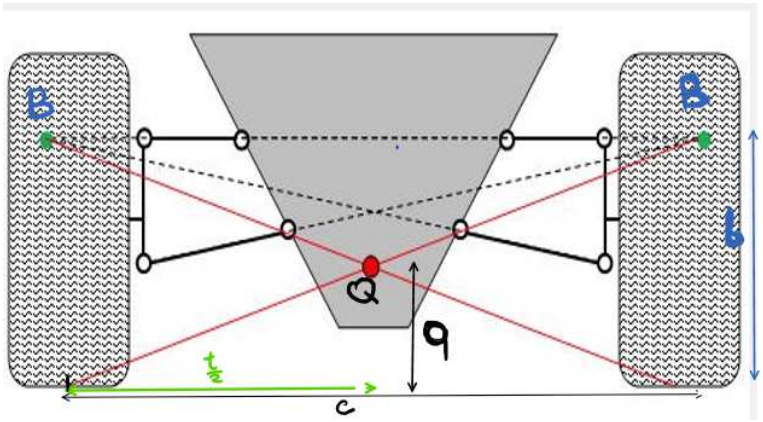

Figure 4.1. Rear axle suspension scheme

Assume that the ground clearance of the car in road configuration is 185mm and that the distance of the attachment joints of the two arms on the car body is 329mm. Under these conditions, figure 4.1 schematizes the resulting geometry in static conditions. The non-parallel nature of the suspension arms and their anchoring scheme to the car body imply all the characteristic quantities are the

following:

TABLE 4.1	
c	18,855 m
b	-0,623 m
t	1,791 m
q	-0.0296 m

The configuration shown in figure 4.1 shows a general configuration fora double wishbone suspension system. It is useful to understand how the Centro of rotation and roll center parameters can be found geometrically. In table 4.1 shows the coordinate "c" and "b", which represent the coordinates along the x and z axis of the centre of rotation "B". Similarly, "q" is the vertical coordinate of the roll centre "Q". The "Q" parameter can be obtained in two ways:

- Geometrically: intersecting the two axes, which represent the extension of the upper and lower arms of the suspension, point B is evaluated. Tracing a line which connect point B with the contact point between the wheel and the ground, and intersecting it with the axis, perpendicular to the ground, passing through the center of the track, the roll center Q is identified.

- Analytically: knowing the distance of the center of rotation with the ground "b",the track "t" and the distance from the contact point of the wheel and the COR "c" , It's possible to evaluate the "q" distance. The mathematical relation is the following:

$$q_z = \frac{tb}{2c} \tag{4.1}$$

  Equation 4.1 holds in static configurations, if the car is rolling the only way to evaluate the roll center is the geometric method.

4.1 Track and camber variation

Once the kinematic parameters have been defined, it is possible to evaluate the variation of the values assumed by the camber and the track as a function of the parameters and other quantities such as the vertical deviation due to the suspension z_s, the roll angle due to the suspension φ^s and the deformation of the tire:z^t, φ^t. The camber angle is the measurement of the angle between the vertical and the center plane of the wheel, observing the vehicle in front and with two wheels in a straight-ahead position, while the track is the distance between the wheel's central contact points, belonging to the same axle.

4.1.1 Camber

The equation that links the variables mentioned above with the camber γ angle turns out to be the following:

$$\gamma = \gamma^0 + \Delta\gamma = \gamma + \frac{\partial\gamma}{\partial\varphi^s}\varphi^s + \frac{\partial\gamma}{\partial z^s}z^s + \frac{\partial\gamma}{\partial\varphi^t}\varphi^t + \frac{\partial\gamma}{\partial z^t}z^t \tag{4.2}$$

The terms are made explicit below:

$$\frac{\partial\gamma}{\partial\varphi^s} = -\frac{t_i/2 - c_i}{c_i} = 0.953 \tag{4.3}$$

$$\frac{\partial\gamma_L}{\partial z^s} = -\frac{1}{C_i} = -0.0530 \tag{4.4}$$

$$\frac{\partial\gamma}{\partial\varphi^t} = 1 \tag{4.5}$$

$$\frac{\partial\gamma}{\partial z^t} = 0 \tag{4.6}$$

Observing the results obtained with equations 4.3 and 4.4, it can be noticed that the car's roll angle during a turn is almost wholly transferred to the wheels' camber angle, resulting in a bad handling configuration. On the contrary, the change in the height of the sprung mass does not involve the camber angle, resulting in a good comfort configuration.

Taking into consideration a test that analyzes the dependence between vehicle body roll and pneumatic camber, it is possible to note that there is an effective concordance between experimental and theoretical data.

To carry out the test, the center of mass of the vehicle body was connected to a "revolute joint". This configuration prevents the vehicle body from moving in a vertical direction, keeping the ground clearance constant and to eliminate all those contributions that could negatively influence the test, like, for example, any unwanted roll off-set. In addition, deformation of the tires was prevented as it could compromise the results obtained. To induce the roll, a step input equal to two degrees is given around the "y" axis to the car body. This forced rotation causes an increase in the tire camber angle. Figure 4.2 shows the roll angle in blue and the camber angle in yellow. The resulting values are shown in the following table:

Analytically evaluating the impact that the roll angle variation has on the camber, it settles at:

$$\gamma = \frac{\partial\gamma}{\partial\varphi^s}\varphi^s = 1.905\ deg; \tag{4.7}$$

TABLE 4.2		
Static Camber: γ^0	-0.06	deg
Final Camber	1.85	deg
Final roll angle	2	deg
Total Camber	1.91	deg

Consequently, comparing the value obtained from the equation 4.7 with the value in table 4.2, it is noted that the value obtained experimentally coincides with the expected data

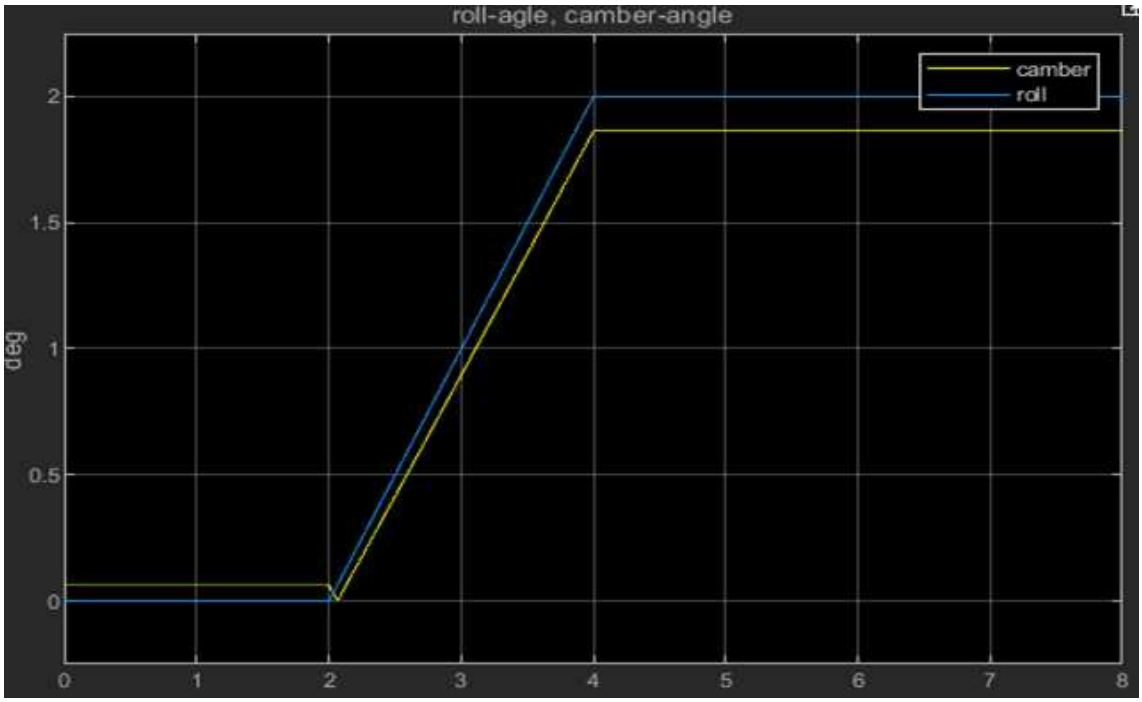

Figure 4.2. Roll and camber angle

Now, evaluating the variation of the camber angle in relation to the vertical lifting of the vehicle using the formula expressed by the relation 4.4. By imposing vertical displacement, thanks to a step signal, of varying amplitude on the vehicle body, the variation in camber of the wheels, calculated analytically, is evaluated using the following relation:

$$\Delta analitic = \frac{\partial \gamma}{\partial z^s} z^s = -0.0530 \Delta z* \tag{4.8}$$

In the next table, the expected values are compared with those obtained through the model:

TABLE 4.3		
Δz	$\Delta \gamma analitic$	$\Delta \gamma model$
0.01 m	0.0303 deg	0.0299 deg
0.02 m	0.0607 deg	0.0545 deg
0.05 m	0.152 deg	0.110 deg
0.1 m	0.303 deg	0.091 deg

From the data shown in table 3, it can be seen that the dependence between model and z is not linear as in the theoretical case, in particular it can be seen that there is an effective relevance between model and theory only for small variations in height (figure 4.3, figure 4.4). Figure 4.5 and figure 4.6 the anomalous behavior is highlighted, showing a reduction of the camber angle, contrary to expectations.

As already mentioned above, the consistency between the analytic computation

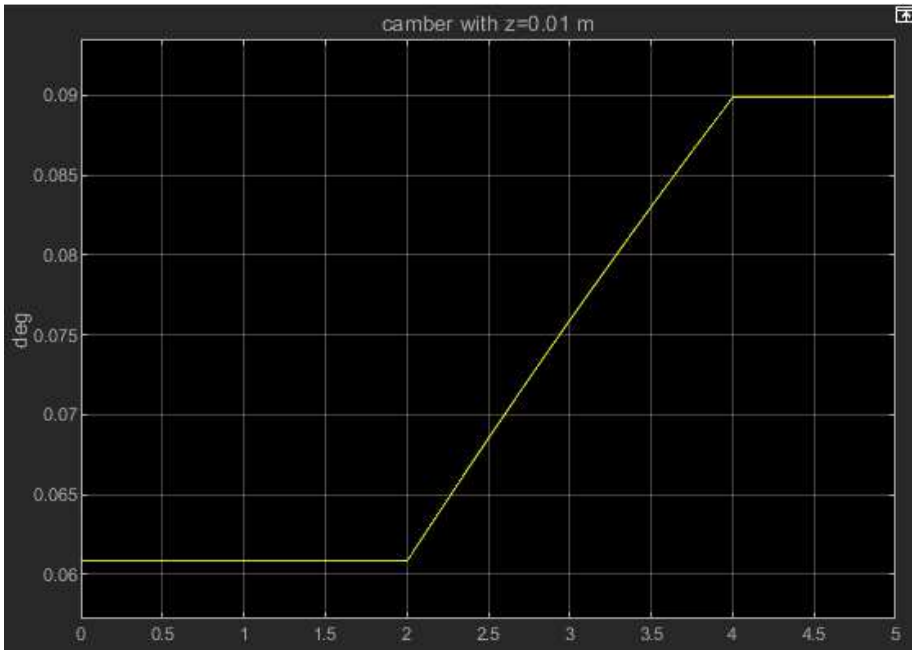

Figure 4.3. Camber angle variation in relation to 0.01 m of vertical displacement

and the results obtained through the Multibody model is present only for small variation od the vertical displacementΔz. Figures 4.5 and 4.6, show a particular behaviour, in fact once a certain threshold is exceeded the camber angle starts to decrease.The possible explanations may be attributable to different factors:

- Geometry of the suspension
- Computational limits of the equation 4.8, due to simplification

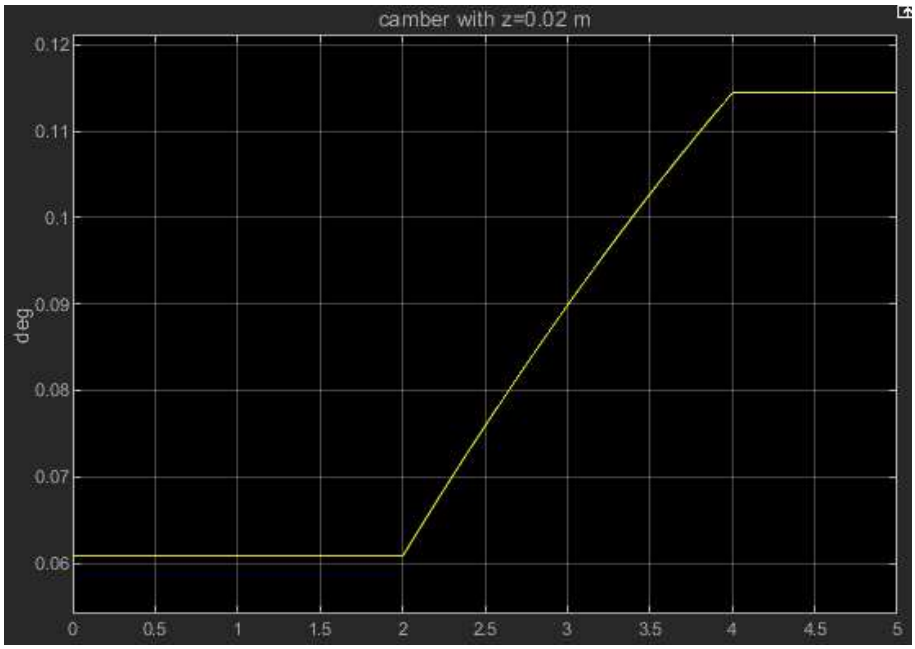

Figure 4.4. Camber angle variation in relation to 0.02 m of vertical displacement

4.1.2 Track variation

It's evaluated how, based on the change in the vertical height of the vehicle, the length of the track varies. Also in this case,the same type of test is carried out, a ramp signal block generates the vertical displacement of the sprung mass and the variation in time of the track is observed. The analytical relationship that measures the difference in deviation is based on the kinematic parameters listed in Table 4.1 .

$$\Delta t = \frac{4q}{t} z^s \tag{4.9}$$

TABLE 4.2.1		
Δz	$\Delta t_{analitic}$	Δt_{model}
10 mm	0.66 mm	0.52 mm
20 mm	1.32 mm	0.9 mm
50 mm	3.31 mm	0.62 mm
100 mm	6.61 mm	-4.17 mm

Like in the previous paragraph, also in this case it can be noticed a concordance between expected values and model values only for small variation in sprung mass height. In particular, the relationship between carriageway and vertical deviation

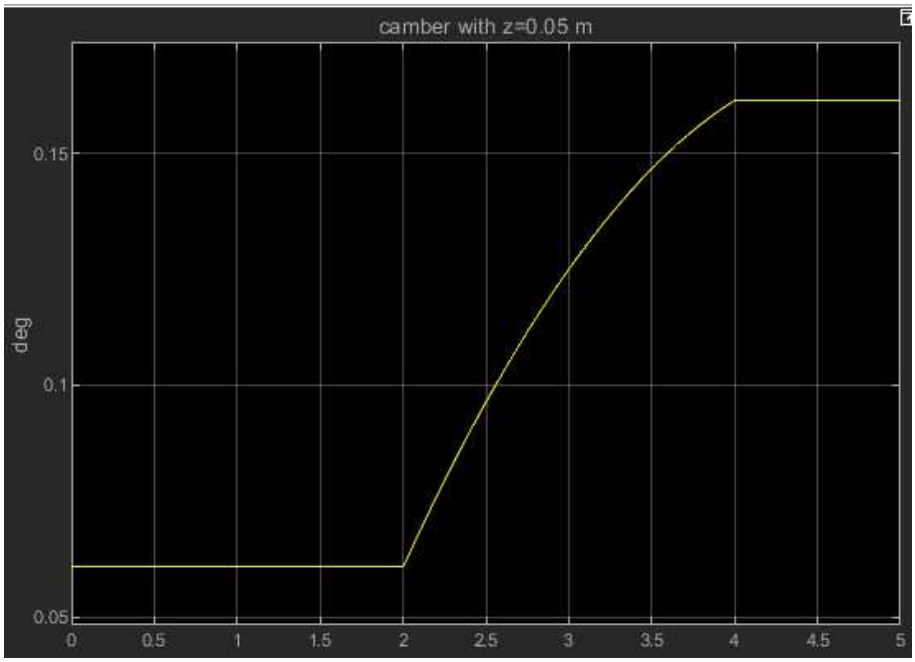

Figure 4.5. Camber angle variation in relation to 0.05 m of vertical displacement

ceases to be linear once a certain threshold is exceeded, however it holds the same type of considerations expressed above.

Next figures(4.7,4.8,4.9,4.10) show the relation between vertical displacement Δz and Δt.

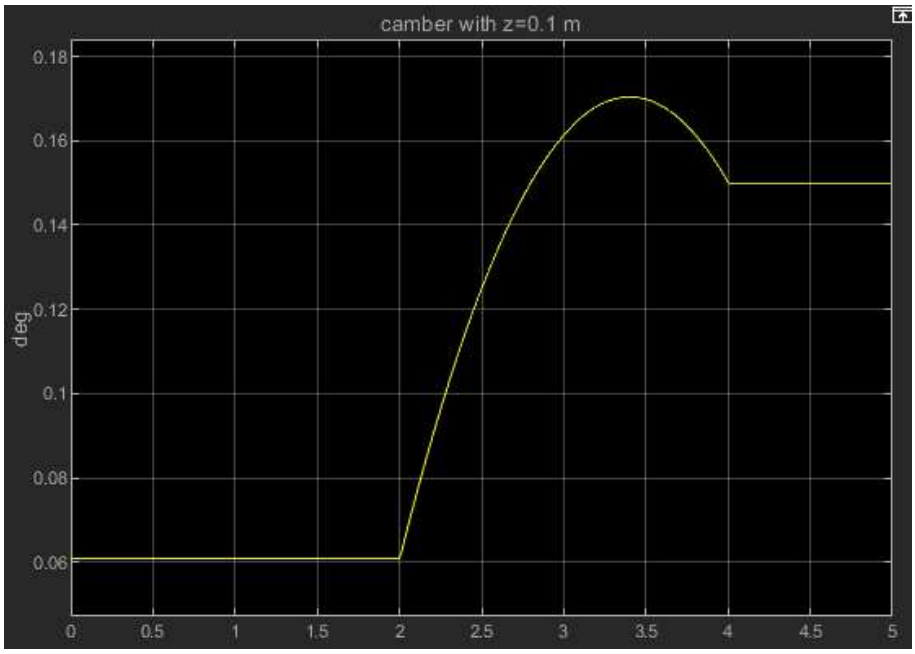

Figure 4.6. Camber angle variation in relation to 0.1 m of vertical displacement

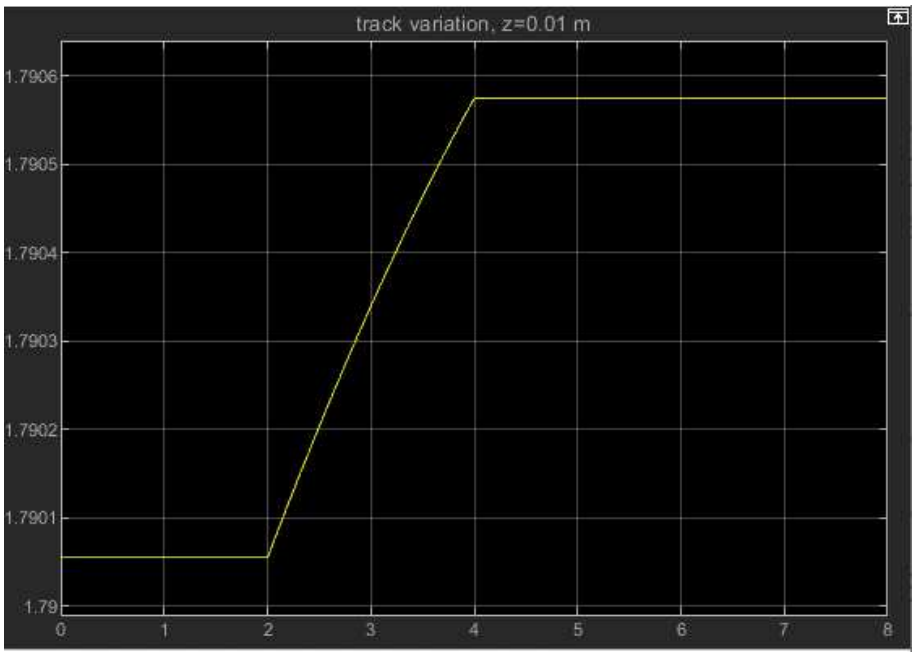

Figure 4.7. Track angle variation in relation to 0.01 m of vertical displacement

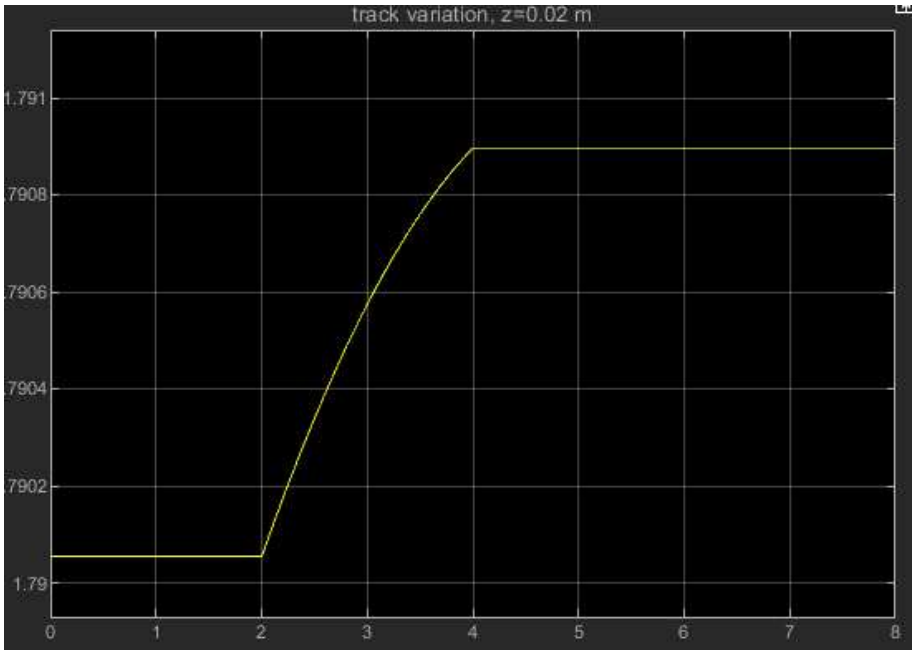

Figure 4.8. Track angle variation in relation to 0.02 m of vertical displacement

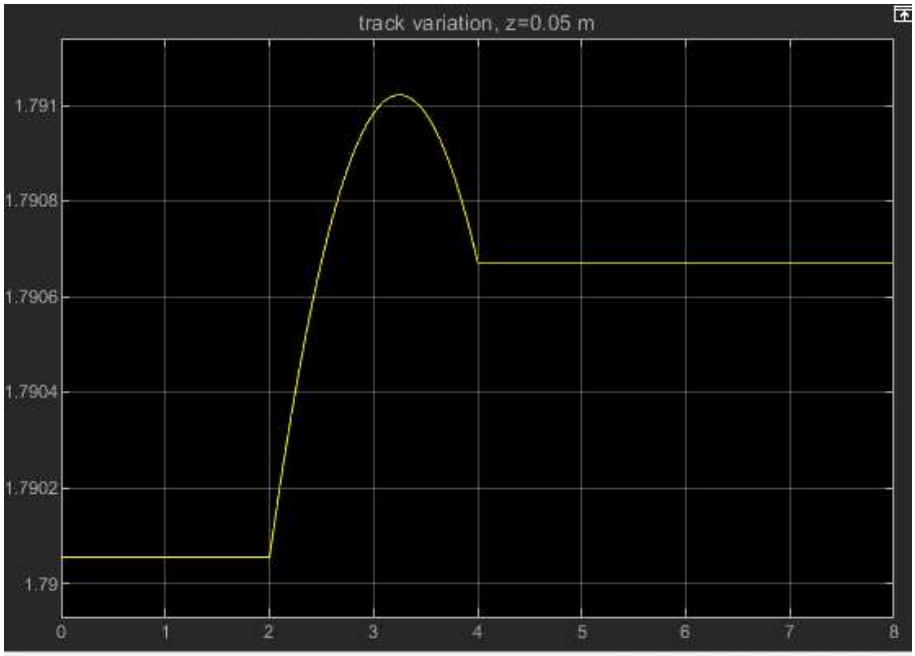

Figure 4.9. Track angle variation in relation to 0.05 m of vertical displacement

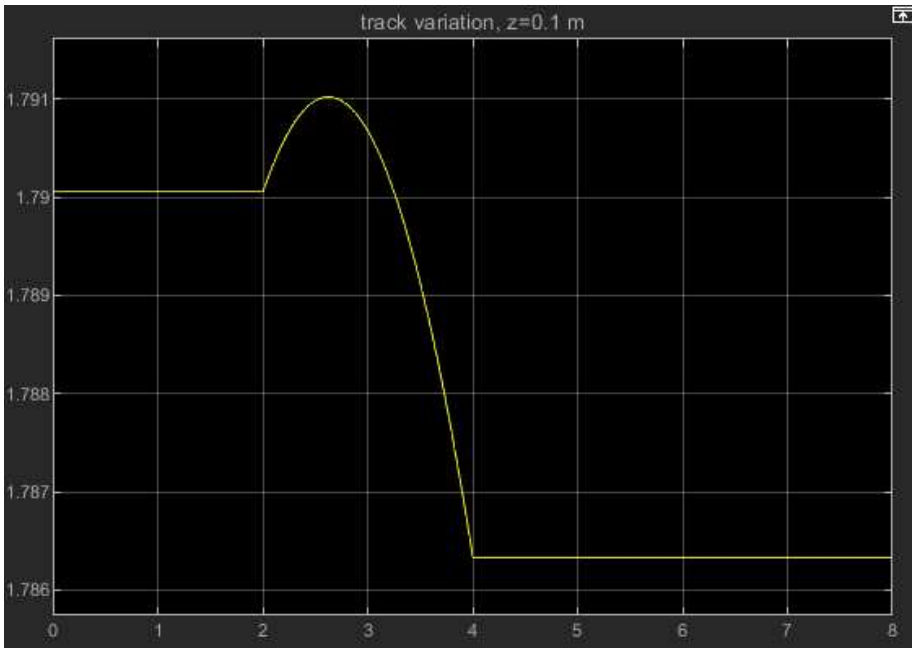

Figure 4.10. Track angle variation in relation to 0.1 m of vertical displacement

4.2 Project and Multibody model: differences

4.2.1 Static condition

Some differences are present between the project presented by the company and the model developed with Multibody: Let's start analyzing the roll centre in the static condition of the two examples. First, it is important to notice the difference between the project, analized through the CAD model of the suspension, and the Multibody Model. The first case is an ideal case, in which the tire deformation is not taken into account and the Q parameter is computed analytically. In the second case , instead, the tire deformation is considered and the Roll centre is evaluated geometrically, creating a CAD scheme of the suspension, sized according to the values extrapolated from the model. The "q" parameter is very sensitive to any changes in sizes of the components, for this reason, a few millimetres of difference lowers the attachments of the suspension arms, resulting in a different suspension configuration. This is clearly shown in table 4.2.1 where it's compared the project configuration without tire deformation and the multibody Model with deformation

The effect of the tire deformation cannot be neglected since the difference between the two models is relevant.

TABLE 4.5			
	B [m]	C [m]	Q [m]
Project model	-0.612	18.855	0.0296
tire deformation	-0.286	26.968	0.0100

4.2.2 Dynamic condition

Three tests are carried out to evaluate the roll centre of the suspension system, each one is performed with different lateral acceleration values: 0 , 0.5 and 1 g of lateral acceleration applied to the vehicle's center of mass. A scheme of the suspension system is recreated using CAD software "CATIA" once all the relevant sizes are noticed. Figure 4.2.2 shows the scheme used to find the position of the roll centre.To find the roll centre, axes are drawn as an extension of the arms of both suspensions and the two centres of rotation B1 and B2 are graphically found. Then the points are connected to the centre of the wheels related to the suspension; check figure 4.1 as reference. The intersection of the two lines determines the roll centre. Once the roll centre is evaluated, the vertical component "q(z)" of Q is computed measuring the distance between Q and the line that represents the ground, while the lateral component "q(x)" is obtained by measuring the distance between the Q and the axis passing at the middle of the car in a static configuration

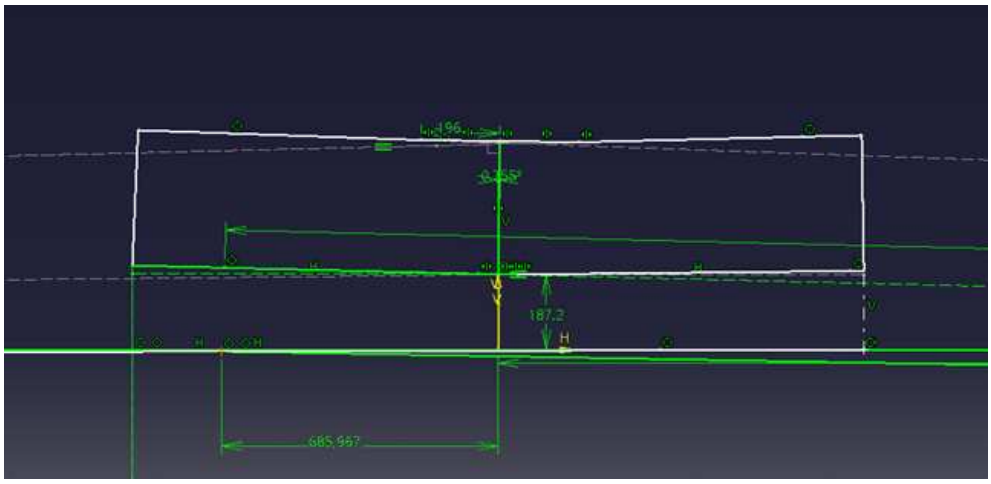

Figure 4.11. CAD scheme of the suspension system

Figures 4.12, 4.13 show the relations between the lateral force applied to the COM during the tests and the roll center movement along vertical and lateral direction.

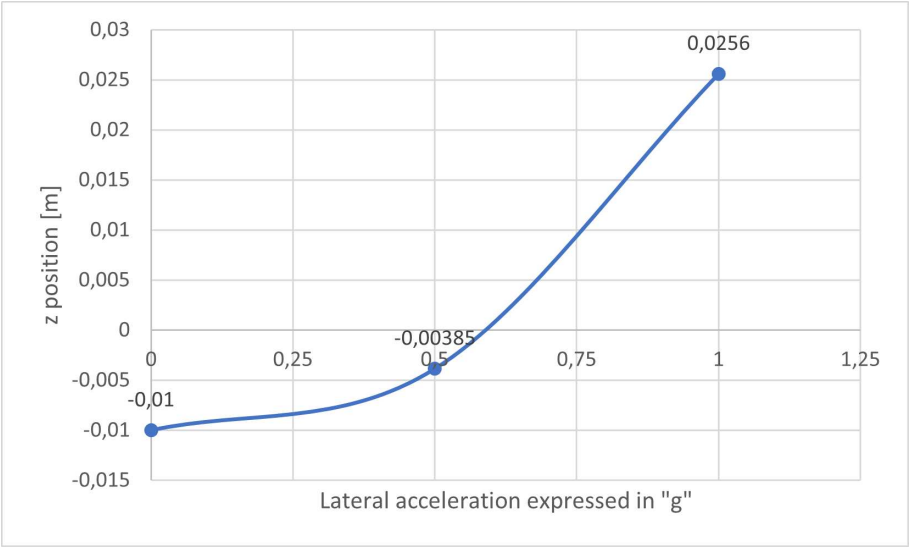

Figure 4.12. Vertical position of the roll centre

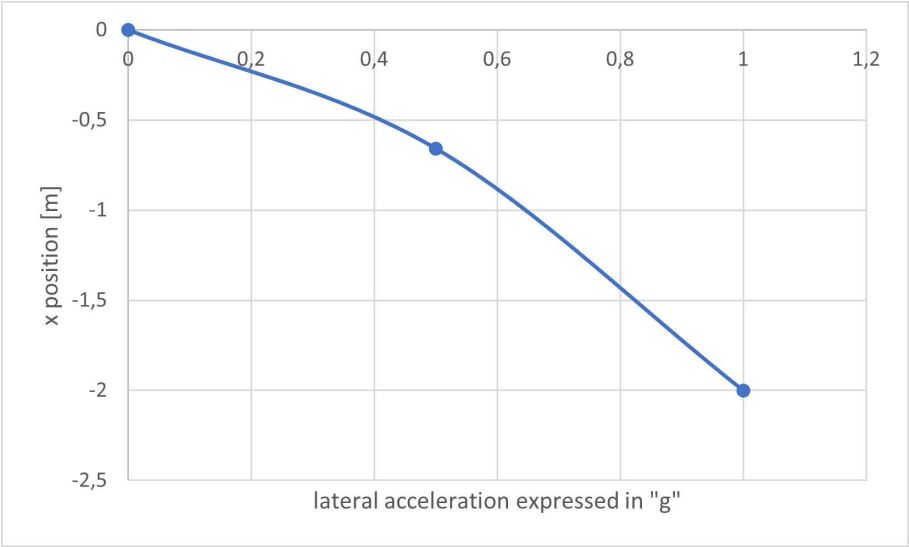

Figure 4.13. Lateral position of the roll centre

Chapter 5

Vertical and roll Stiffness analysis: sensitivity of the hydraulic circuit

This chapter describe the process that led to the creation of the Multibody model having the characteristic required by the company. The main goal is to develop an interconnected suspension system for a high-performance SUV, having specific characteristics in terms of vertical and roll stiffness, listed below:

- Roll angle demand:1.5 degrees of roll angle for each "g" of lateral acceleration applied to the car centre of mass.
- Vertical stiffness demand: ride frequency of the rear suspension equal to 1.5 Hz, which is the oscillation frequency considering the sprung mass acting on the wheel

The frequency demand of the company, related to a single degree of freedom system, is composed of one mass attached to a single spring (figure 5.1). The following system represents the quarter car model containing only the sprung mass of the vehicle, a spring and a shock absorber.

The equation characteristic of the system for a generic n-degrees of freedom, expressed in matrix form, is the following:

$$[M]\ddot{z} = -[C]\dot{z} - [K]z \tag{5.1}$$

Since it's considered only an one degree of freedom System , without the shock absorber, the the resulting equation is:

$$[M]\ddot{z} = -[K]z \tag{5.2}$$

the solution of equation 5.2 can be expressed as:

$$z(t) = Z_0 cos(\omega t + \phi) \tag{5.3}$$

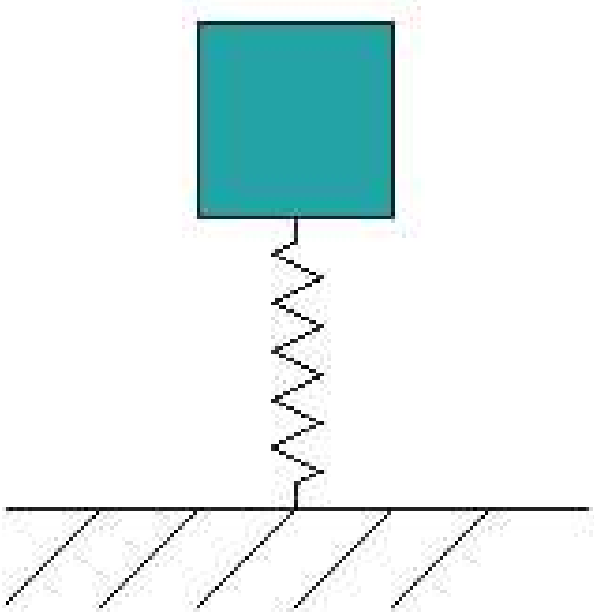

Figure 5.1. Quarter car model: single degree of freedom

where X_0 is a constant non-zero vector, deriving an substituting 5.3 into 5.2, it is obtained the following relation:

$$-\omega^2[M]X_0 cos(\omega t + \phi) + [K]X_0 cos(\omega t + \phi) \tag{5.4}$$

which leads to:

$$X_0([K] - \omega^2[M]) = 0 \tag{5.5}$$

The eigenvalue problem, here proposed, lead to the evaluation of the natural frequencies of a n-degree of freedom system. The solution is obtained computing the determinant of equation 5.6:

$$det([K] - \omega^2[M]) = 0 \tag{5.6}$$

In this case, the one degree of freedom system has one natural frequency, related to the sprung mass. The vertical stiffness is derived to have the model with the required characteristic. Imposing the natural frequency of the sprung mass, equal to 5.7, having f=1.5 Hz, the natural frequency is computed:

$$\omega = 2\pi f = 9.42 \frac{rad}{s}; \tag{5.7}$$

Considering that the model which is going to be developed represents the rear axle of the vehicle, the weight considered is half of the body's car, whose weight is approximately 2000 Kg, so in this case, 1000 Kg. Once angular frequency is derived, the wheel rate results to be equal to the mass acting on a wheel multiplied by angular frequency squared:

$$K_w = M\omega^2 = 500 * 9.42^2 = 44413\frac{N}{m} \tag{5.8}$$

This value represents the wheel rate, which is the vertical stiffness measured at the wheel instead of where the spring is attached to the linkage. To estimate the spring rate is necessary to derive the motion ratio of the suspension, which is the ratio between the wheel displacement and the spring displacement:

$$MR = \frac{WheelDisplacement}{SpringDisplacement}; \tag{5.9}$$

A vertical displacement is applied to the wheel and the resulting spring displacement is observed and listed in table 5.1. Once the motion ratio is obtained, the spring stiffness is calculated, through the following relation:

$$K_s = K_w MR^2 \tag{5.10}$$

TABLE 5.1

Wheel Displacement	Spring Displacement	MR	Ks
0,05	0,0294	1,701	128457
0,1	0,0593	1,685	126129,6
0,15	0,0899	1,669	123754,8

As can be seen from table 5, the motion ratio is not constant due to the geometry of the suspension system, the direct result is the non-constant value of the spring's stiffness, for this reason, an average of all the values related to it is applied. The resultant spring stiffness is: $K_s = 126114\frac{N}{m}$

Once the spring stiffness is defined it's possible to apply this parameter to the model resembling the real geometry of the suspension system. Figure 1 It's shown the suspension scheme made using the Multibody toolbox: The mechanical system, presented in figure 5.2, is coupled to a hydraulic system connected in parallel to the suspension springs. This hydraulic system aims to reduce and prevent the rolling behavior of the body's car. The system is composed of two hydraulic actuators, which substitute the classic shock absorbers, two gas-charged accumulators, and two local resistances.

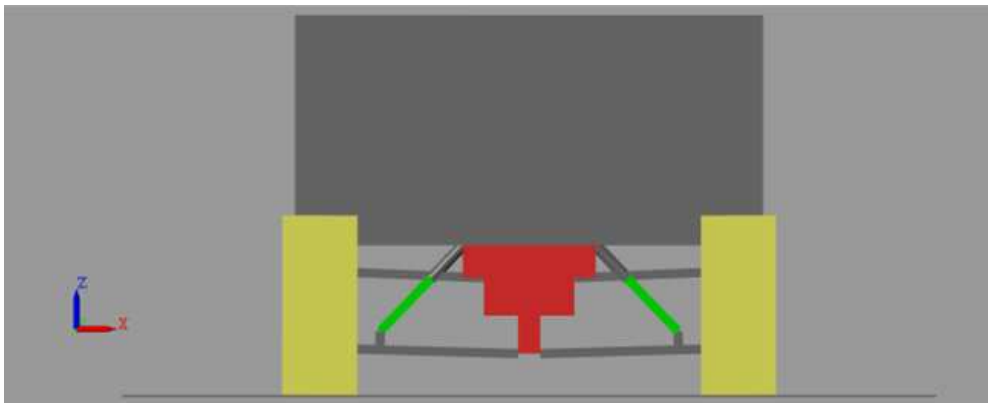

Figure 5.2. Multibody rear axle scheme .

5.1 Sensitivity analysis

To get the performance required by the Company, once the suspension scheme is fixed, all the parameters that characterize the hydraulic circuit are studied. All the parameters considered listed below are divided according to the hydraulic components.

Gas-charged accumulator

- V: The accumulator's total volume, including the fluid chamber and the gas chamber. It is the sum of the fluid chamber capacity and the minimum gas volume.
- P: Pressure (gauge) in the gas chamber when the fluid chamber is empty.
- Vliq: Volume of fluid in the accumulator at time zero. Simscape software uses this parameter to guide the initial configuration of the component and model. Initial variables that conflict with each other or are incompatible with the model may be ignored. This parameter can be enabled or ignored

Local resistance

- Rs: radius of the resistance area.

Hydraulic actuator

- AR: area of the piston chamber.
- Ar: area of the piston rod.

TABLE 5.2		
V	0.5	l
Vliq	disabled	l
P	70	bar
Rs	2	mm
R	25	mm
r	7.5	mm

For this kind of analysis, a default configuration is chosen, while during the test a variable is modified maintaining the others constant. In this way, we can easily detect which are the variables that affect the most the performance of the vehicle. The default configuration is described in table 5.2: The analysis is carried on applying a force in the center of mass of the vehicle along the lateral direction, causing the vehicle to roll.

In the next figures, the direct dependence between the roll angle and the variables considered is shown:

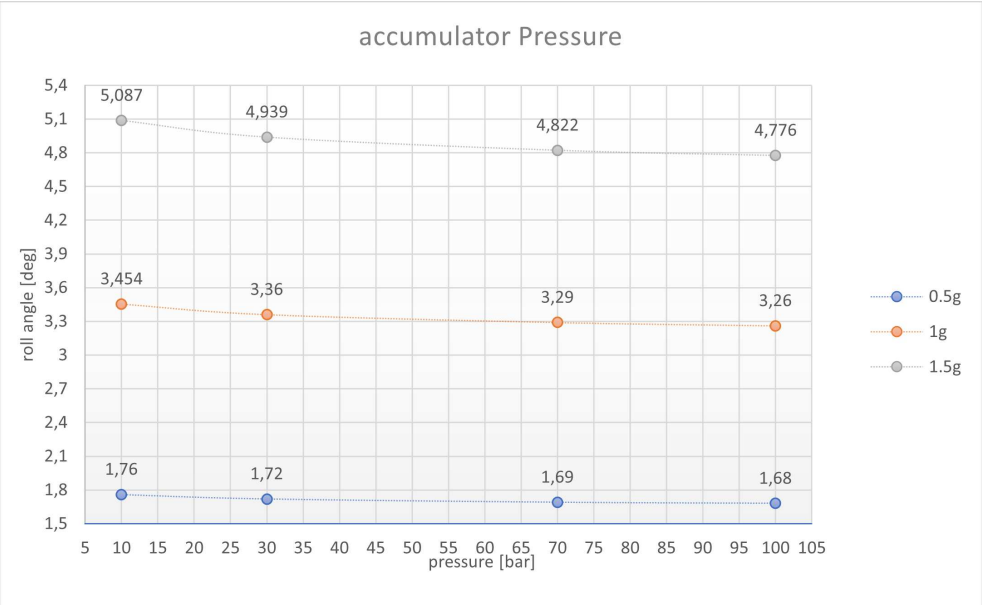

Figure 5.3. Accumulator pressure/Roll angle .

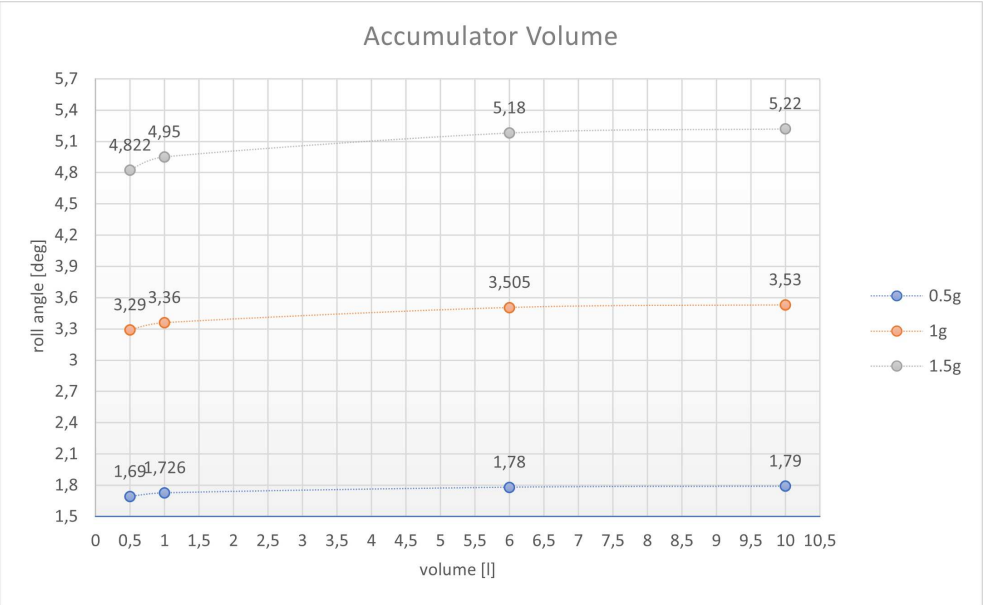

Figure 5.4. Accumulator volume/roll angle

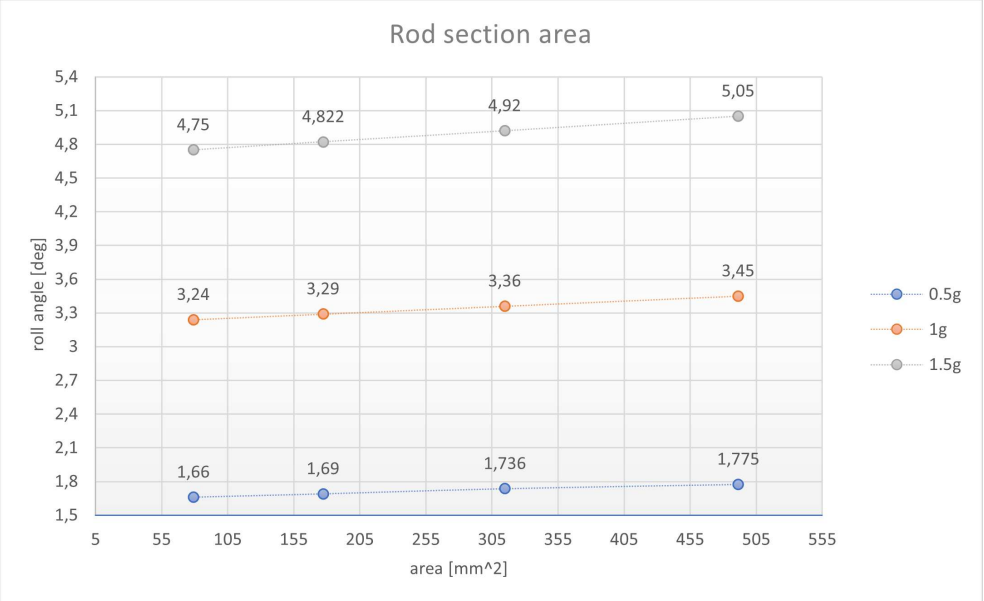

Figure 5.5. Rod section area/ Roll angle

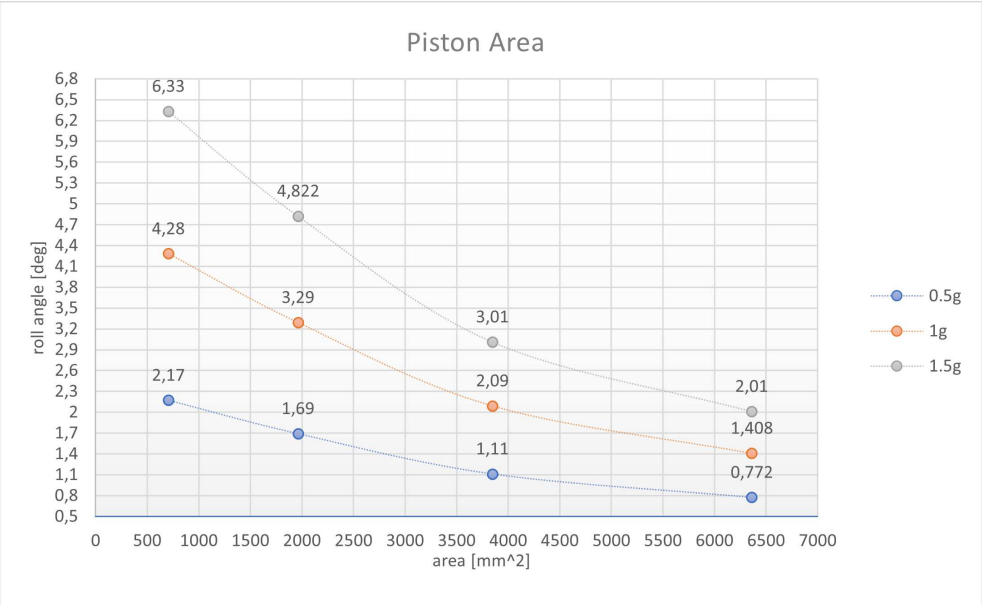

Figure 5.6. Piston Area/Roll angle

As shown by the figures 5.3 5.4 5.5 the parameters have a mild influence on the roll angle, on the contrary, the piston area has an important effect, in fact, it can be noticed that increasing this parameter the roll angle decrease (figure 5.6). Another important parameter that is not considered in the previous cases is the volume of liquid. The reason behind the choice of ignoring it is related to long simulation times. having the parameter disabled, the solver will automatically set a certain quantity of liquid volume inside the accumulator to have an efficient simulation with the shortest possible times. However, once the variable is enabled the solver will force the variable into the equation characteristic of the system trying to not generate dangerous conflict that will lead to long simulation time. Figure 5.7 is shown the direct correlation between the roll angle and the liquid's volume percentage with respect to the total volume accumulator. The results presented above are obtained by setting the other variables with the default setting shown in table 2, with the only exception of variable Vliq.

The results shown in figure 5.7 are not negligible and , moreover, the choice of ignoring The Volume of liquid can lead to dangerous situation. It has been noticed, in fact that inside the liquid chamber of the gas-charged accumulators the liquid pressure becomes negative during the tests, causing cavitation. For this reasons, it's important to find a compromise between fast simulation time and simulation accuracy. Including the volume of liquid, the simulation will be more accurate, however, the main drawback is the difficulty in finding the right solver configuration that allows performing the test in a few minutes.

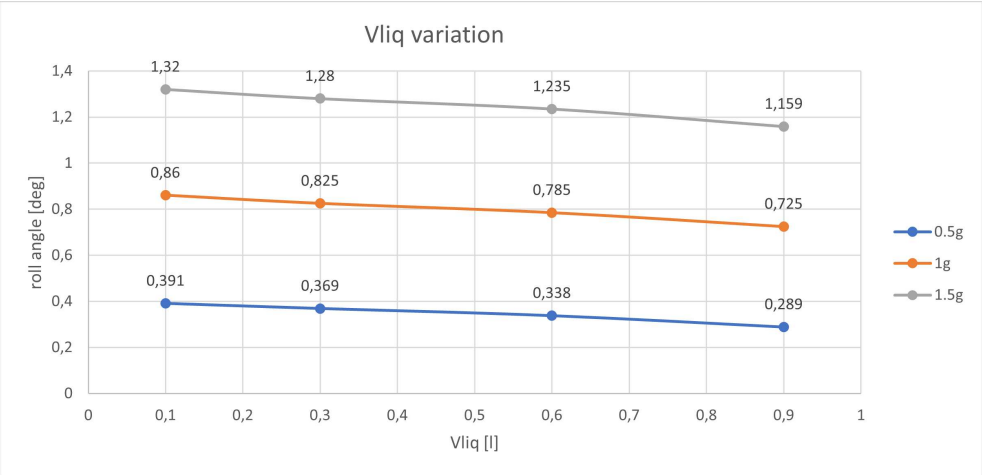

Figure 5.7. Piston Area/Roll angle

5.2 Vertical stiffness

In this section, two different models with different specifics will be compared and analyzed. Two different tests will be performed:

- **vertical parallel travel**: the body's vehicle is blocked and a vertical displacement is applied to both wheels contact point and the couple of forces is measured. These forces are parallel and equal in magnitude. This test is done to evaluate the vertical stiffness calculated at the wheel. Vertical forces are measured in several tests performed applying different displacement, then vertical stiffness is computed:

$$K_p = \frac{F}{\Delta z} \tag{5.11}$$

- **Vertical opposite travel**: the body's vehicle is blocked and, in this case, a vertical opposite displacement is applied at the contact point of the wheels to the wheel having the same magnitude but opposite directions. Several tests are performed with increasing displacement and the the vertical forces of the two suspensions are evaluated.

$$K_{ol} = \frac{F_l}{\Delta z_l}, K_{or} = \frac{F_r}{\Delta z_r} \tag{5.12}$$

These terms are then averaged to obtain K_O

5.2.1 Model 1: Vliq disabled

The configuration of parameters that allows to obtain the rolling target of 1.5 degrees for each "g" of lateral acceleration is shown in table 5.3: Once the correct

TABLE 5.3		
P	70	bar
V	0,2	l
R	50	mm
r	5	mm

configuration is found vertical parallel and opposite travel test were performed. In both cases the methodologies are similar, the vehicle body is fixed and only the wheels are actuated. A step input signal provide force to the contact point of the wheels. The only difference between the two tests consists on the sign of the forces, which are equal for the vertical parallel test while, in opposite travel, are opposite in magnitude.

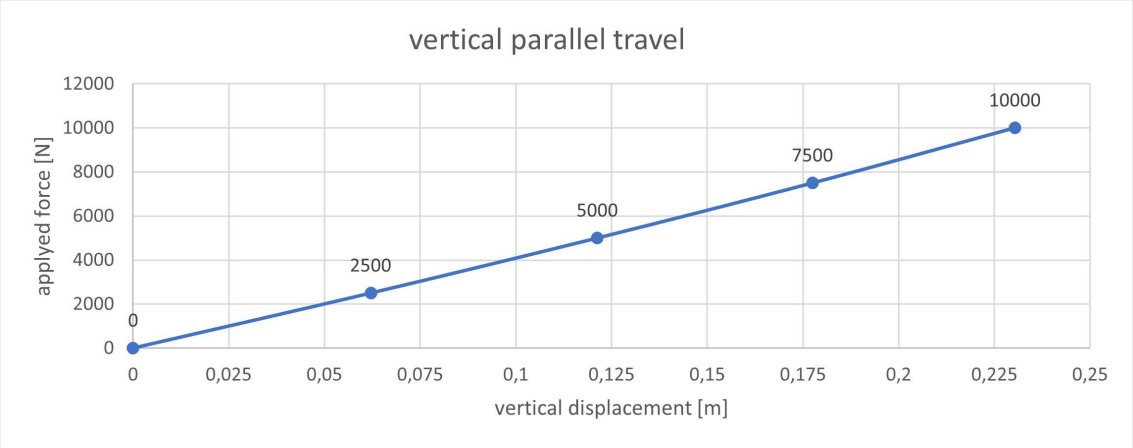

Figure 5.8. Vertical parallel travel

Figure 5.8 shows the relation between the vertical displacement of the wheel and the applied force, which is almost linear. The angular coefficient, which represents the parallel stiffness, is computed for each point of interest and then reported in the chart shown in figure 5.9. It's interesting to underline that the stiffness is not constant but slightly increases raising the absolute value of the force. The vertical

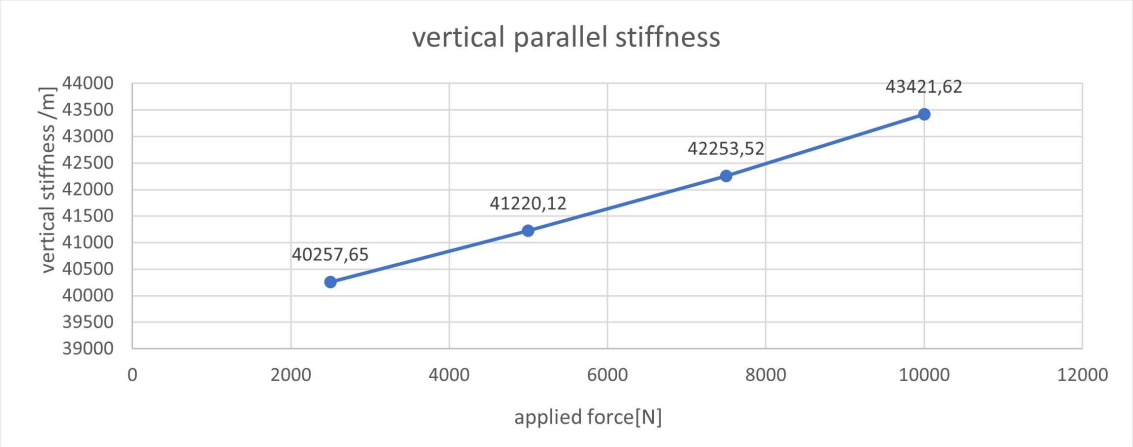

Figure 5.9. Vertical parallel stiffness

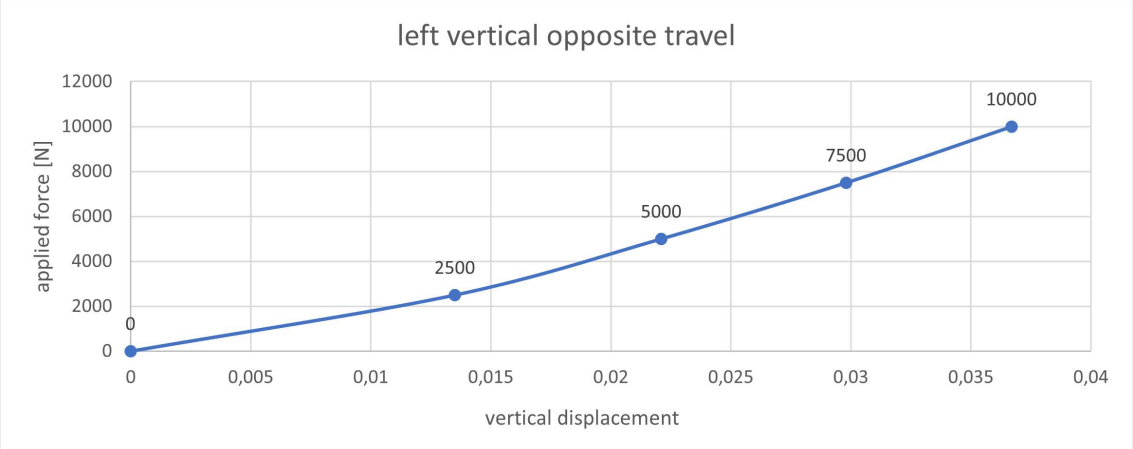

Figure 5.10. Left vertical opposite travel

parallel stiffness is then computed by averaging the obtained values:

$$K_p = 41788\frac{N}{m} \tag{5.13}$$

It's important to underline that the value computed above is close to the theoretical wheel rate computed in the first paragraph. The same procedure is applied to vertical opposite travel analysis, as shown below:

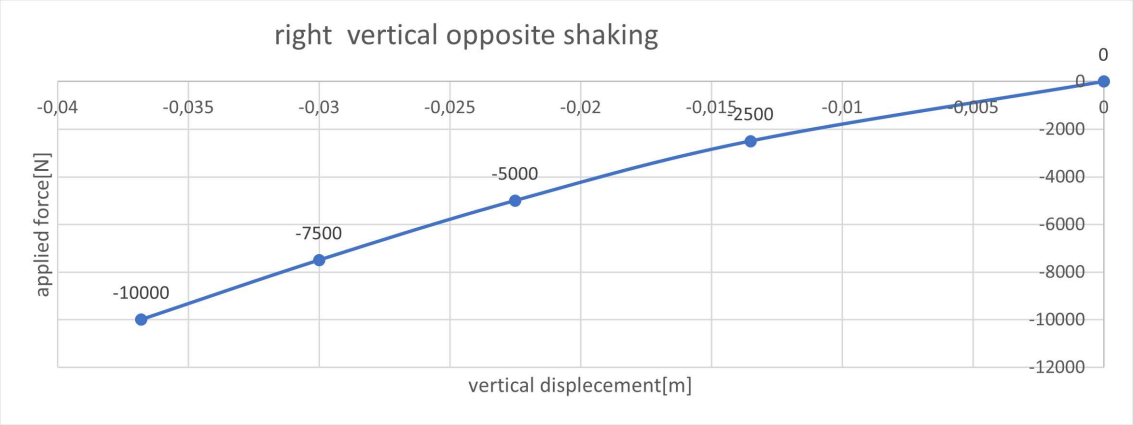

Figure 5.11. Right vertical opposite travel

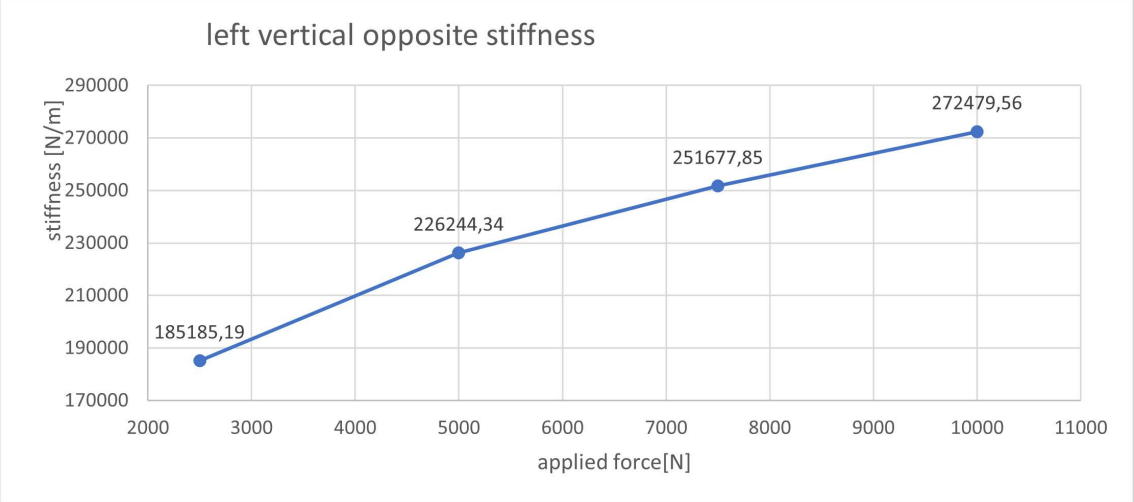

Figure 5.12. Vertical opposite stiffness

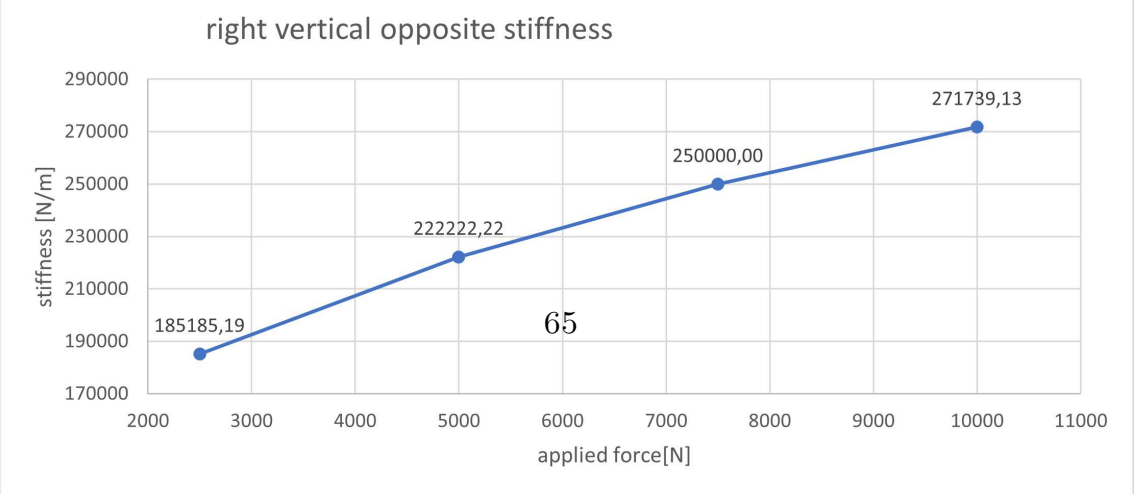

Figure 5.13. Vertical opposite stiffness

Figure 5.10 and figure 5.11 show the relation between the applied forces and the vertical displacement of the wheels and, unlike in the previous case, the linearity is not maintained.

The charts show that the bigger the imposed force is, the bigger the vertical stiffness will be, and also in this case the non-linearity of the system is shown. The values are averaged between left and right stiffness and the following result is obtained:

$$K_o = 233091 \frac{N}{m} \tag{5.14}$$

5.2.2 Model 2: Vliq enabled

The second model developed has the following characteristic dimensions:

TABLE 5.3		
V	0.2	l
Vliq	0.5V	l
P	50	bar
Rs	1	mm
R	28	mm
r	7.5	mm

The same procedure applied for Model 1 is now carried out for Model 2. It can be noticed that the obtained results are comparable.

Figure 5.15 shows that the vertical parallel stiffness is the same as in the previous case, figure 5.9. It is possible to approximate that the rolling behaviour is linear, resulting in a parallel stiffness almost constant. The values of the chart in figure 5.15 are averaged and, as already pointed out, the expected wheel rate :

$$K_p = 41847 \frac{N}{m} : \tag{5.15}$$

Once again, the same procedure is carried out to vertical opposite travel analysis, shown above:

Figure 5.16 and figure 5.17 show the relation between the applied forces and the vertical displacement of the wheels. The vertical stiffness for each point of interest is computed and its behaviour is presented in figures 5.18 and 5.19:

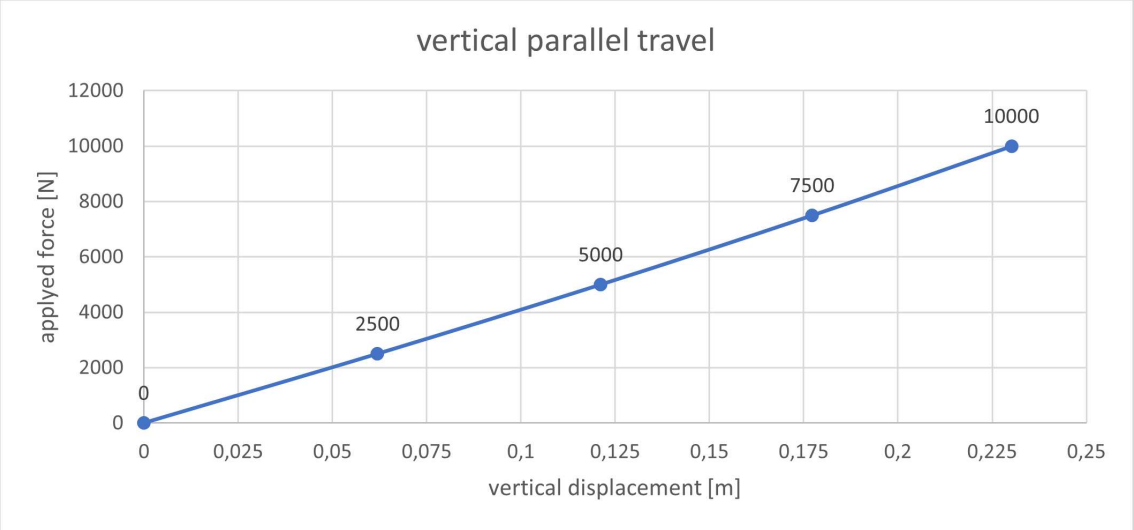

Figure 5.14. Vertical parallel travel

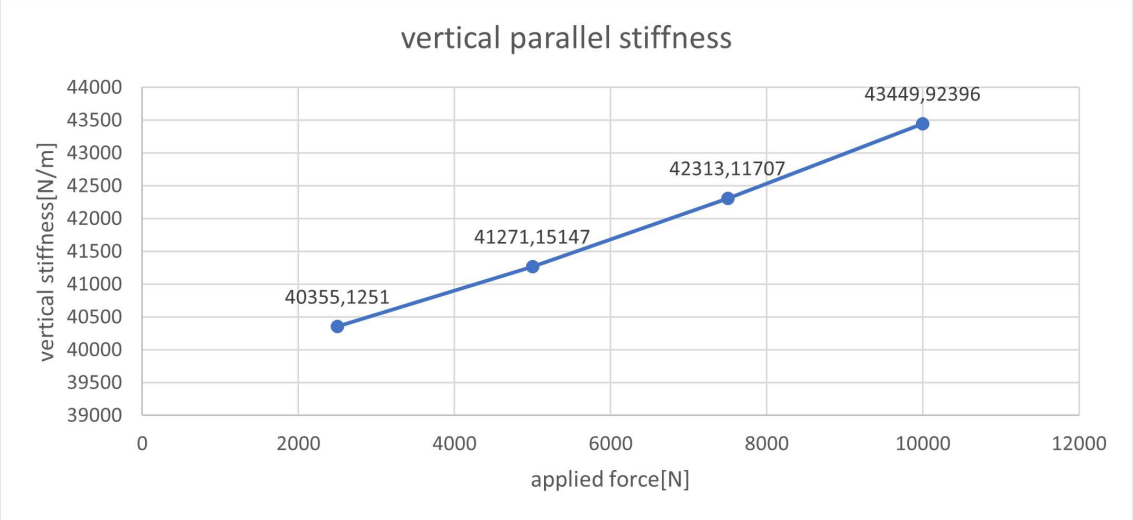

Figure 5.15. Vertical parallel stiffness

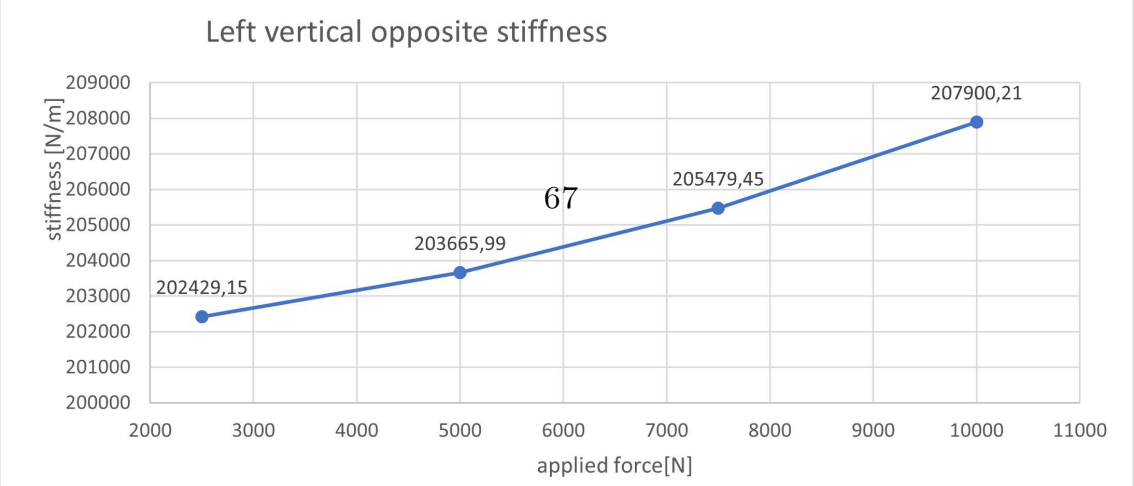

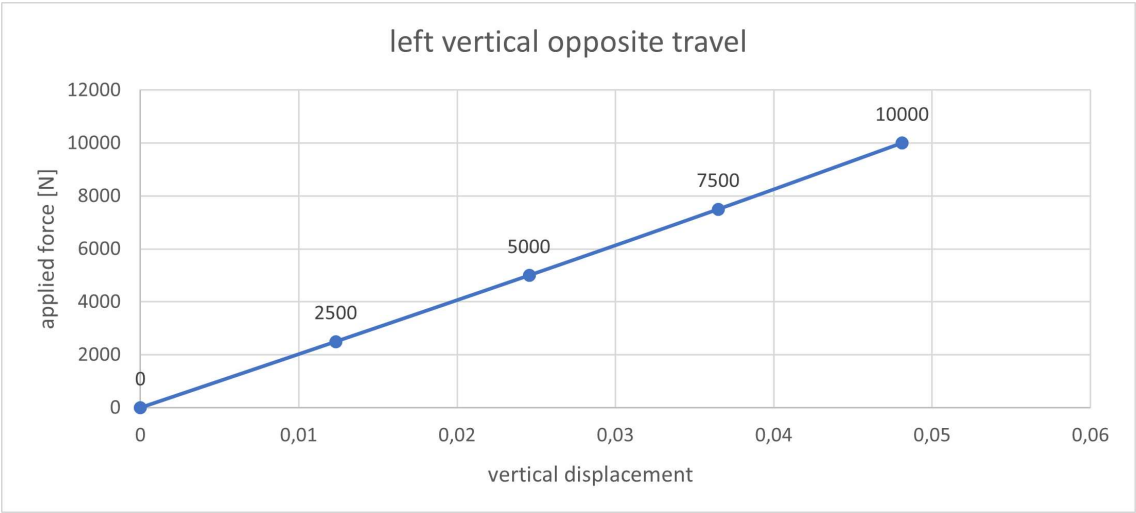

Figure 5.16. Left vertical opposite travel

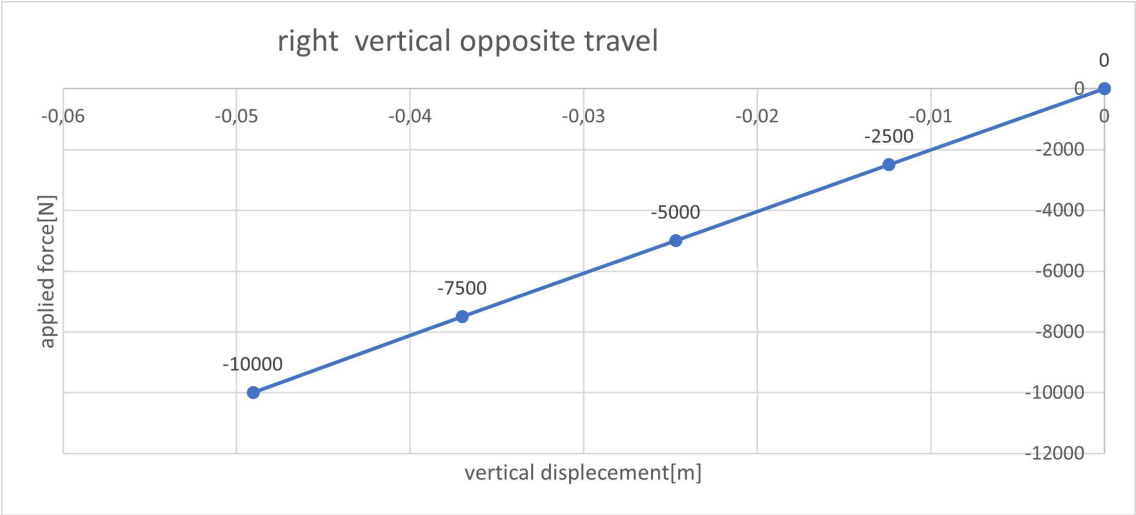

Figure 5.17. Right vertical opposite travel

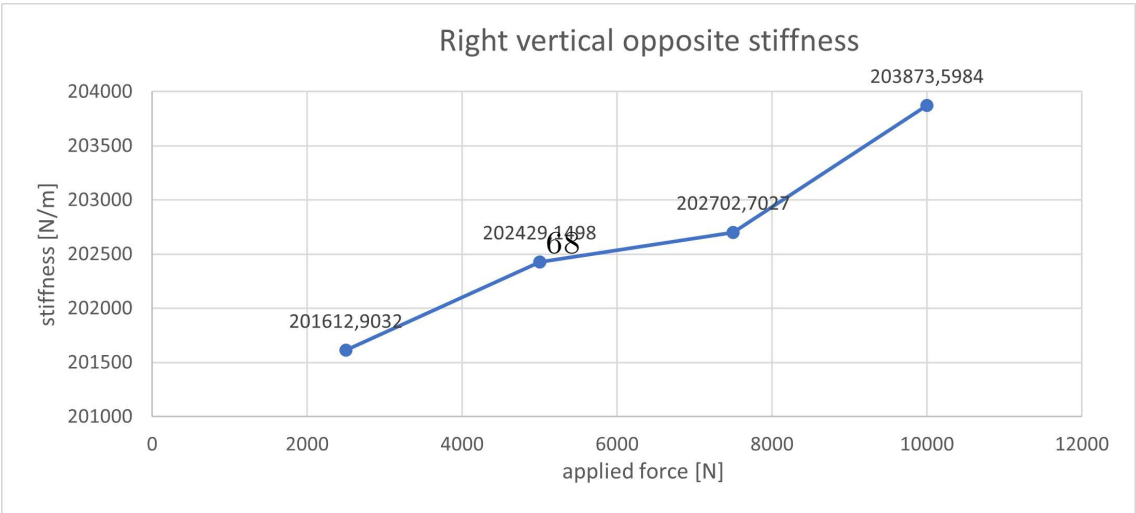

As it is possible to notice by observing figure 5.18 and figure 5.19, the values of the vertical opposite stiffness are almost constant. The slight difference between the left and right sides may be attributed to the data extrapolation process, which is done manually; for this reason, it can be prone to errors. However, since the difference is negligible in absolute value, these parameters are averaged:

$$K_o = 203091 \frac{N}{m} \tag{5.16}$$

5.2.3 Results comparison

The results show a slight difference between the two models, as illustrated in the table.

TABLE 5.4		
	Model 1	Model 2
K_o	233091 N/m	203091 N/m
K_v	41788 N/m	41847 N/m

Both exhibit comparable vertical stiffness; however, the first model exhibits slightly higher opposing shaking stiffness. During the simulations, it was seen how the pressure of the liquid that fills the chamber of the gas-charged accumulator is negative, figure 5.20.The volume of liquid inside the accumulator strongly impacts the simulation results. It is noted that, with the same characteristics of the hydraulic system, in particular the size of the hydraulic actuator, the results are better. In addition, deactivating the volume of liquid inside the accumulator, it places itself in dangerous situation, since it starts in empty condition. Thus, by the configuration proprieties of the gas-charged accumulator, if the volume of liquid at any time is zero, the pressure inside the accumulator is also zero. Consequently, during the simulation the discharging accumulator has Vliq drops, leading to negative pressure. This behaviour is dangerous because it can lead to cavitation therefore, model 2 is chosen.

5.3 Natural frequency evaluation

One of the main requests is to develop a physical system of one degree of freedom having a natural frequency $f = 1.5Hz$. The natural frequency belongs to the vehicle's sprung mass; the computation lead to defining the elastic coefficient of the spring for the 1 degree of freedom system and, consequentially, the elastic coefficient of the model presented in figure 5.2. To verify the correct behaviour of the system, two simulations are carried out: the first without the hydraulic circuit and the second with the system enabled. The model presented above is

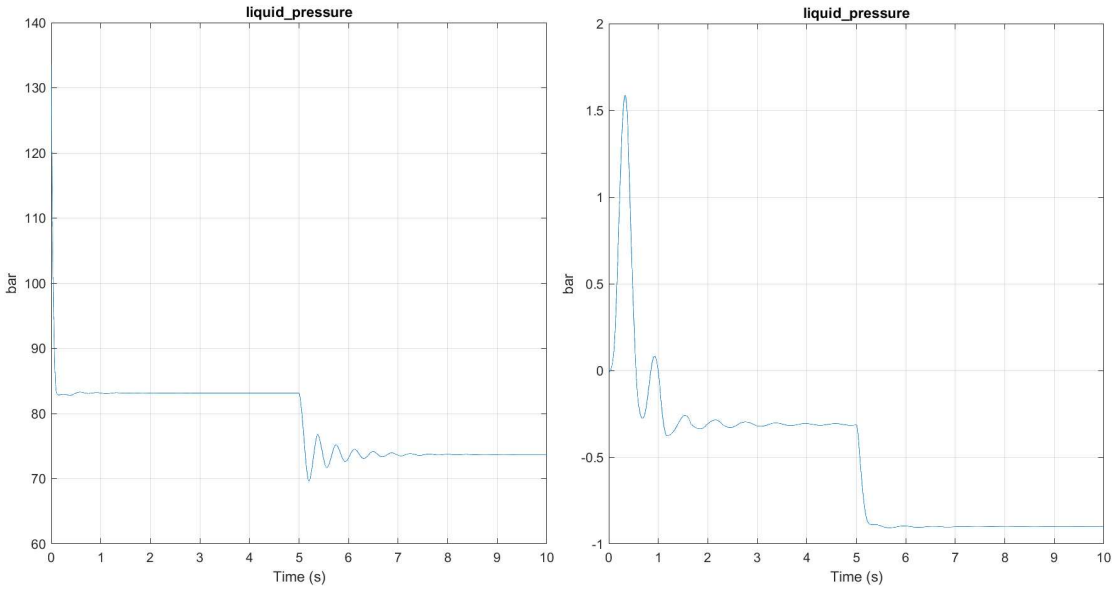

Figure 5.20. Liquid pressure model 2 vs model 1 in the gas charged accumulator

slightly modified to consider only the sprung mass contribution, so the tires are considered non-deformable. Blocking the vertical displacement of the wheels, the model studied becomes a single degree of freedom system. The car's body is only able to move in the vertical direction and is unable to roll.

In this section, it will demonstrate the actual natural frequency of the system to see if the model, here analyzed, comply with the demand of the company. The oscillatory behaviour of the system is evaluated once an external input is applied to the wheels. A vertical displacement is applied through a step input and the base position of the car's body is observed. Two cases are analysed:

- **Hydrauic circuit disabled**: obtained by removing the hydraulic circuit responsible for the dissipation of energy due to the damping characteristic of the system. In this configuration, the car's body oscillates freely.The oscillation's period and the frequency are evaluated directly from figure 5.21,$T = 0.6702s$ and $f = 1/T = 1.492Hz$, from the graph and the natural frequency is computed as follows:

$$\omega_{n1} = 2\pi f = 9.37rad/s; \tag{5.17}$$

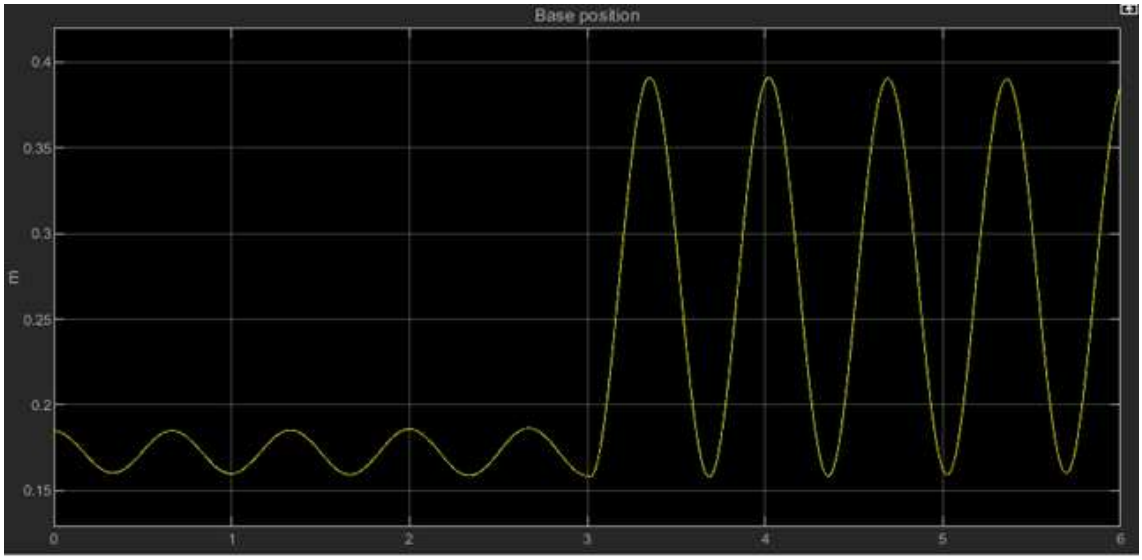

Figure 5.21. free responce of the undamped system

- **Hydrauic circuit enabled** The same procedure of the previous case is carried on. In figure 5.22, the response of the system is shown:

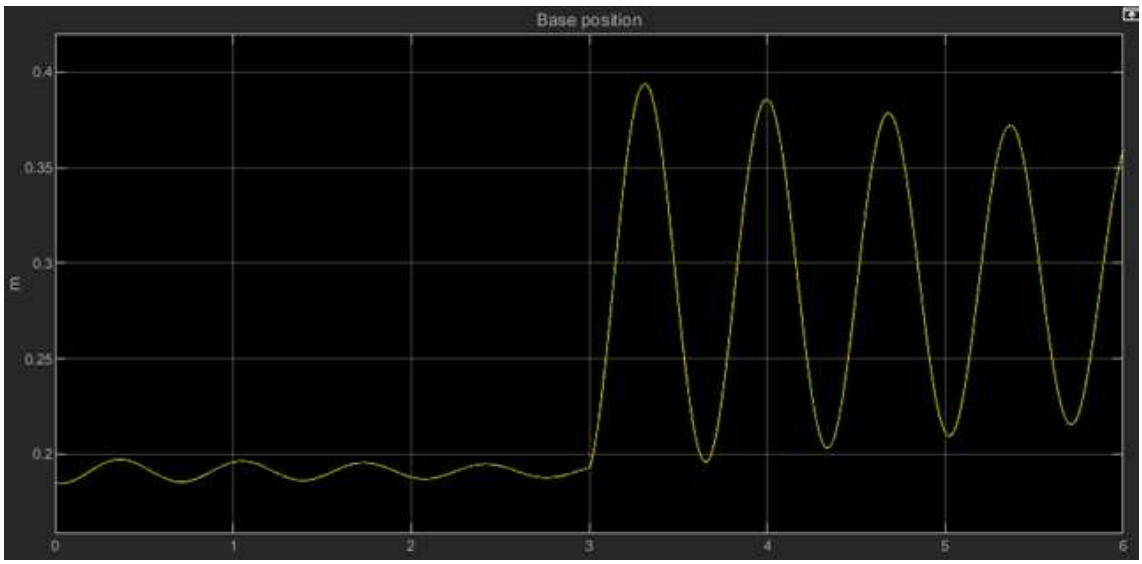

Figure 5.22. Free responce of the damped system

In this case, the system is damped by the action of the hydraulic circuit having a local resistance with a radius of 5 mm, the oscillation's period and the frequency are evaluated directly from figure 5.22,$T = 0.681s$ and $f = 1/T = 1.468Hz$, from the graph and the damped frequency is computed as follows:

$$\omega_{d2} = 2\pi f = 9.22rad/s; \tag{5.18}$$

5.4 Roll stiffness

In this section, it will be evaluated the the roll behaviour of the car. First, it is essential to consider the roll stiffness of the suspension system. The roll stiffness is the ratio between the torque generated by the suspension's springs and the roll angle of the car. The total torque of the system is computed by multiplying the difference of the force acting on the centre of the wheels with the semi-track of the car, as shown below:

$$T = \frac{t}{2}(F_r - F_l) \tag{5.19}$$

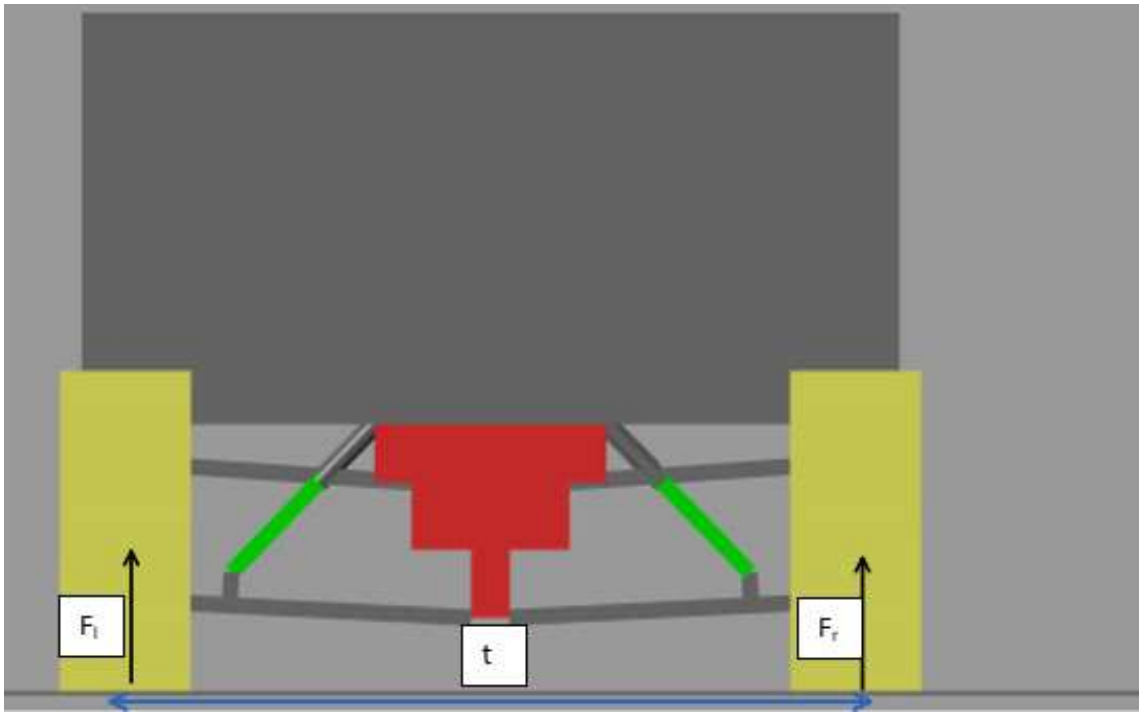

Figure 5.23. Force acting on the ground in static configuration

The computed torque is a function of the roll angle. It has two different contributions: the elastic one, depending on the suspension's springs, and the dynamic one, depending on the force generated by the hydraulic circuit when the rolling velocity is different from zero. To decouple the two contributions a positive and negative constant rotation velocity is applied to the body, verifying the stiffness of the suspensions in both directions. This angular velocity tends to zero, so it is possible to evaluate only the torque generated by the suspension's springs T_{spring}. Figure 5.24 shows how the total torque varies increasing the roll angle.

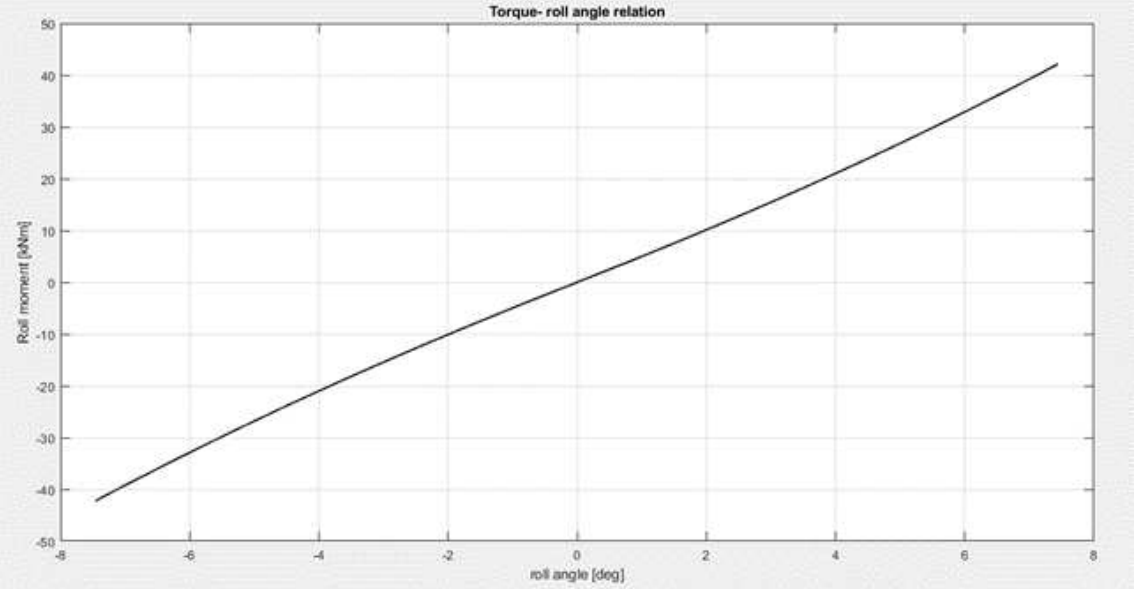

Figure 5.24. Relation between computed torque and roll angle

Knowing the characteristic shown in figure 5.24, the resulting roll stiffness computed by the following relation is:

$$K_{roll} = \frac{T}{rollangle} \tag{5.20}$$

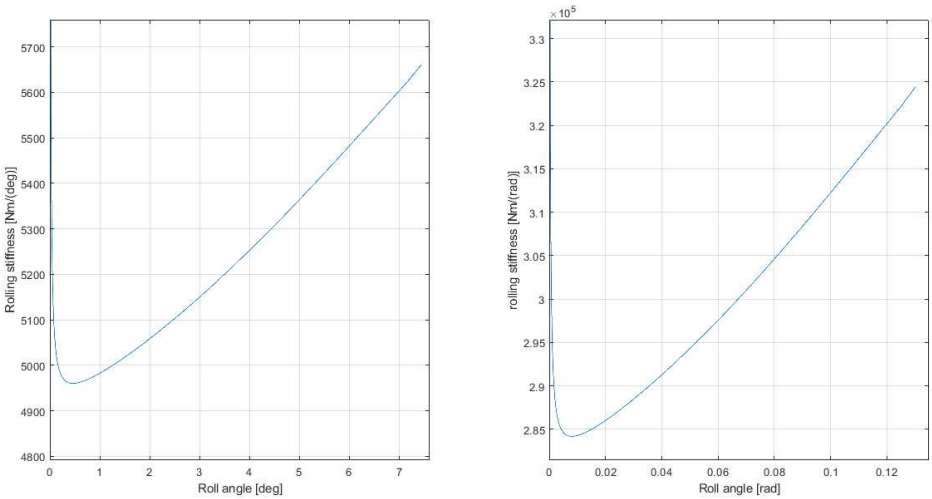

Figure 5.25. Roll stiffness

Figure 5.25 shows the non-linearity of the rolling stiffness, it continues to increase as the roll angle becomes bigger.

Given that the car can sustain lateral accelerations equal to a maximum of 1.2g when cornering, it is essential to define the operating range. For this reason, the relationship between lateral acceleration and roll angle is shown in figure 5.26 and the relationship between the roll angle and roll stiffness is highlighted in figure 5.27.

The values listed in figure 5.27 are averaged, the values related to angles that tend to zero are neglected. Eventually, all the data related to vertical parallel, vertical opposite and roll stiffness are listed in table 5.4

TABLE 5.5		
K_v	K_o	K_{roll}
41874 N/m	203091 N/m	5015 Nm/deg

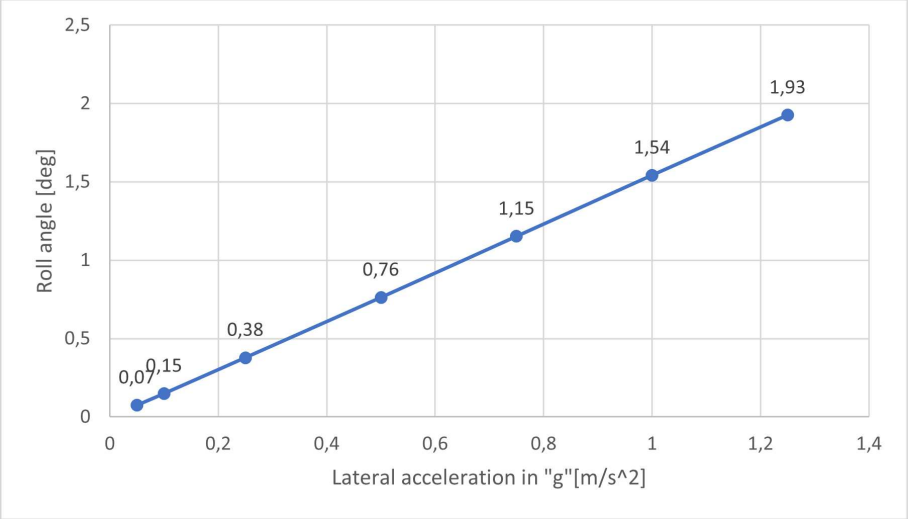

Figure 5.26. Relation between lateral acceleration in "g" and roll angle

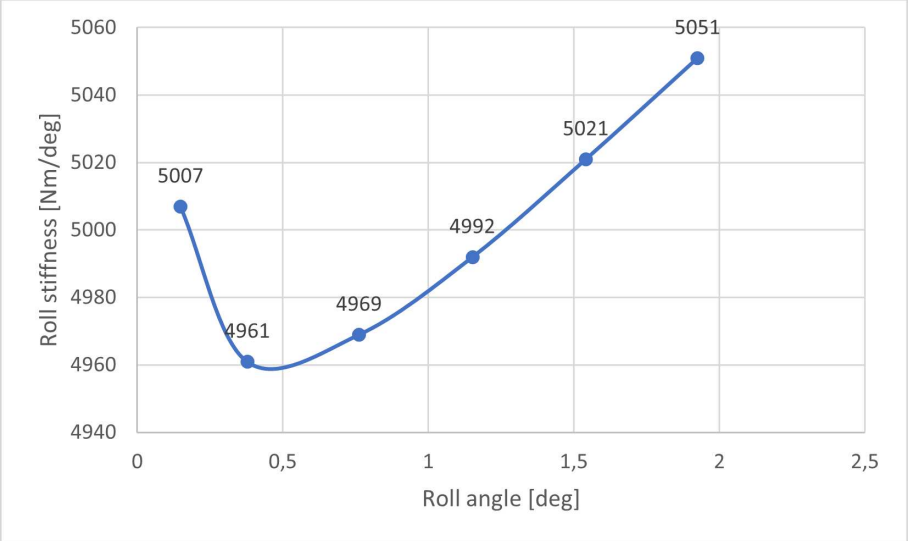

Figure 5.27. Relation between roll stiffness and roll angle

Chapter 6

Damping characteristic of the suspension system

This chapter discusses of the vertical and roll damping characteristic of the suspension system. Like in chapter 5, a sensitivity analysis of the hydraulic system is carried out to find the best configuration in terms of damping performances. It is observed that the damping behaviour of the systems depends on two different components of the hydraulic circuit: the actuator radius and the local resistance radius. Since the piston radius cannot be changed considering the fact that it is tuned to achieve the stiffness target, the only parameter adjustable is the local resistance section. Based on the results achieved in terms of vertical damping characteristic and the analysis of the natural frequency of the sprung mass, the correct section is chosen. In the second part, the roll damping characteristic is evaluated in accordance to the previous results .

6.1 Vertical Damping Characteristic

Several tests are performed to assess the hydraulic resistance section's impact on the system's damping characteristic. The test methodology follows: a vertical offset input is provided to the wheels, and the damping factor is calculated, thanks to the logarithmic decrement method. The logarithm decrement method is useful for computing the damping ratio of an underdamped system, when the ratio is below the 0,5, beyond this value, the method cannot be applied. From the observation of the motion over time of the sprung mass, figure 6.1 it is possible to obtain the quantities necessary for calculating the damping factor, such as the oscillation period and the peaks amplitudes. . The mathematics expression used to compute is the following:

$$\delta = \frac{1}{n} \ln \frac{x(t)}{x(t + nT)} \tag{6.1}$$

where $x(t)$ is the overshoot peak amplitude and $x(t + nT)$ is the peak after n oscillation period. Once the logarithm decrement is evaluated the damping ratio of the system is evaluated:

$$\zeta = \frac{1}{\sqrt{(1 + (\frac{2\pi}{\delta})^2)}} \tag{6.2}$$

Anothe strategy to compute ζ is by the gollowing relationship:

$$\zeta = \frac{c}{c_{crit}} \tag{6.3}$$

Where c_{crit} is the critical damping coefficient computed as : $c_{crit} = 2\sqrt{mK}$, in this case m is the mass of the body and k is the spring stiffness. The vertical stiffness of the system is constant so, the critical damping is expected to be constant, leading in a constant damping factor for the chosen hydraulic configuration. In this particular case, the logarithm decrement method is applied to two consecutive peaks, so the relation number 6.1 becomes:

$$\delta = \ln \frac{x(t)}{x(t + nT)} \tag{6.4}$$

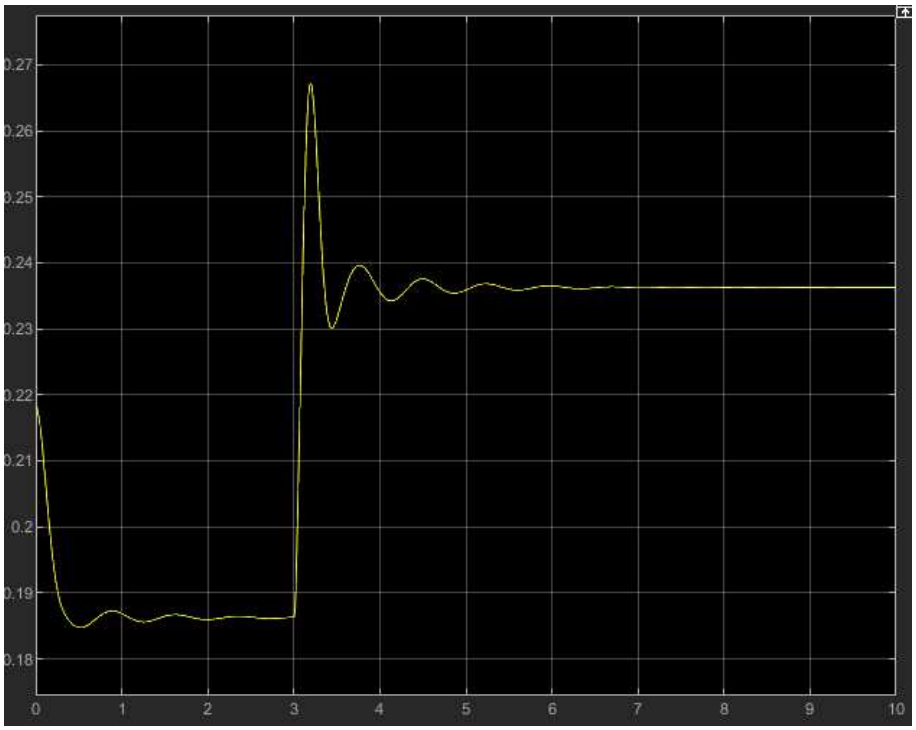

Figure 6.1. sprung mass motion

From the knowledge of these parameters it is also possible to obtain the natural frequency ω_n and the damped natural frequency ω_d of the system.

$$\omega_d = \frac{2\pi}{T} \tag{6.5}$$

$$\omega_n = \frac{\omega_d}{\sqrt{1-\zeta^2}} \tag{6.6}$$

6.1.1 Sensitivity analysis

The following section is intended to describe the relationship between the section size of the hydraulic resistance and the damping factor. Each test, as already explained, is carried out by imposing a vertical displacement on the wheels and observing the motion of the sprung mass. The parameters, such as: logarithm decrement, damping factor and natural frequencies are evaluated and listed in table 6.1.1: The data contained in table 6.1.1 are plotted in figure 6.1.1; as it can be seen,

TABLE 6.1.1

	T	DL	DR	fd [Hz]	fn [Hz]
rs=0,5mm	0,375	0,909	0,143	2,66	2,69
rs=0,75 mm	0,375	1,365	0,212	2,66	2,72
rs=0,9 mm	0,406	1,774	0,272	2,46	2,56
rs=1,0 mm	0,569	1,952	0,297	1,75	1,84
rs=1,1 mm	0,663	1,860	0,284	1,51	1,57
rs=1,5	0,736	1,011	0,159	1,36	1,38
rs=2 mm	0,732	0,533	0,084	1,37	1,37

the trend of damping factor is maximum when the local resistance has a radius of 1 mm.The bell shape of the curve can be traced back to the motion of the fluid inside the resistance. In fact, it can be noted that as the section becomes smaller the damping factor increases, after the maximum value the trend is inverted and the damping factor begins to drop drastically. One of the cause of this behavior may be the transition between laminar and turbulent motion

The value chosen as the radius of the local resistance is equal to 1.1 mm. This choice is due to the good damping value and the system's natural frequency, which reflects the request given by the company, as it possible to observe from table 6.1.1.

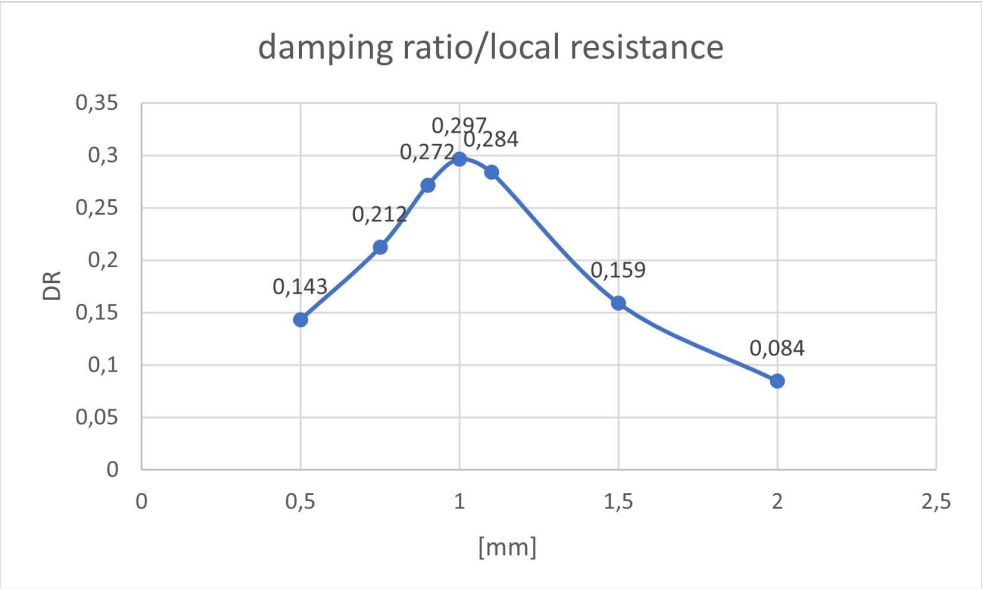

Figure 6.2. sprung mass motion

6.2 Roll damping behaviour

In this section, it is analyzed the suspension's roll damping characteristic when subjected to an external force applied to the vehicle's centre of mass.

In the previous chapter, it was described how to compute the torque related to the spring's action, computed by rotating the centre of the vehicle's body with an angular velocity close to zero. On the contrary, in this case, the body is rotated with increasing velocity for each test carried out, in order to evaluate the contribution of the torque related to the damping characteristic.

To decouple the two contributions, the first related to the springs and the second one related to the damping action of the suspension, the following computation is performed:

$$T_{dam}\,(deg) = T\,(deg) - T_{spring}(deg) \tag{6.7}$$

The torque related to spring action, figure 5.24 is subtracted from the total torque value, calculated according to the relationship 5.19, obtaining the desired contribution. Let's take, for example, the case with a constant angular velocity equal to 5 [deg/s]. The roll characteristic of the system is expressed in figure 6.2

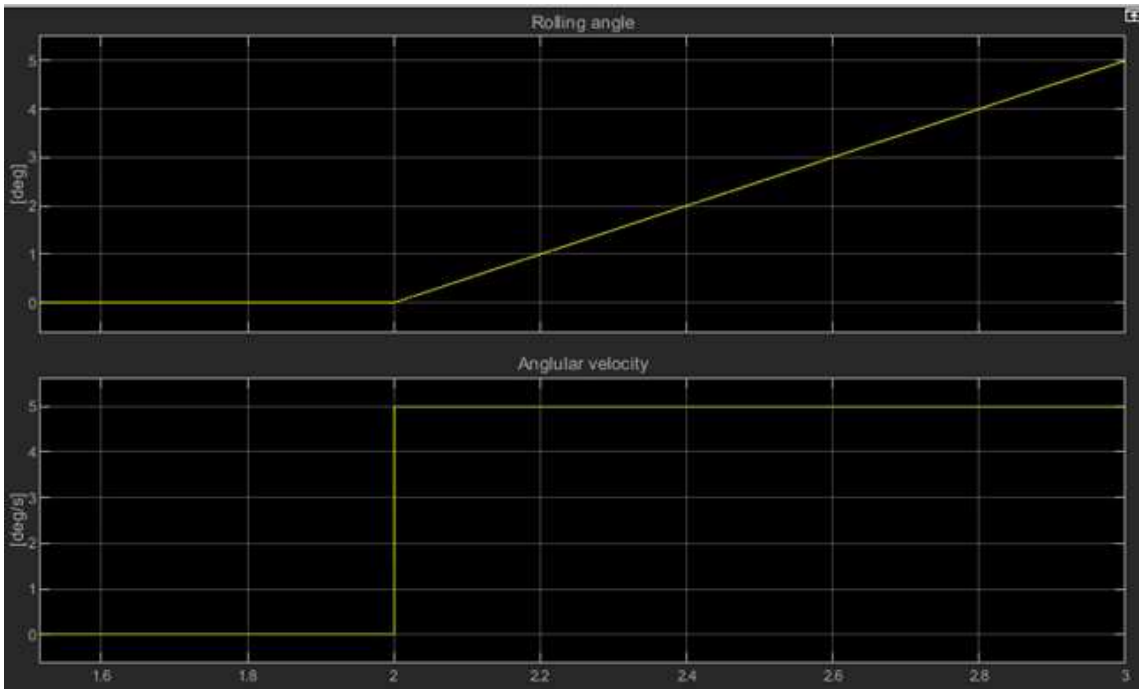

Figure 6.3. Roll characteristic with constant angular velocity

The total torque generated by a couple of forces acting on the centre of the wheels is shown in figure 6.2. As mentioned above, the torque related to the spring's action (figure 5.24) is subtracted and eventually, the damping torque is finally computed, as shown in figure 6.2.

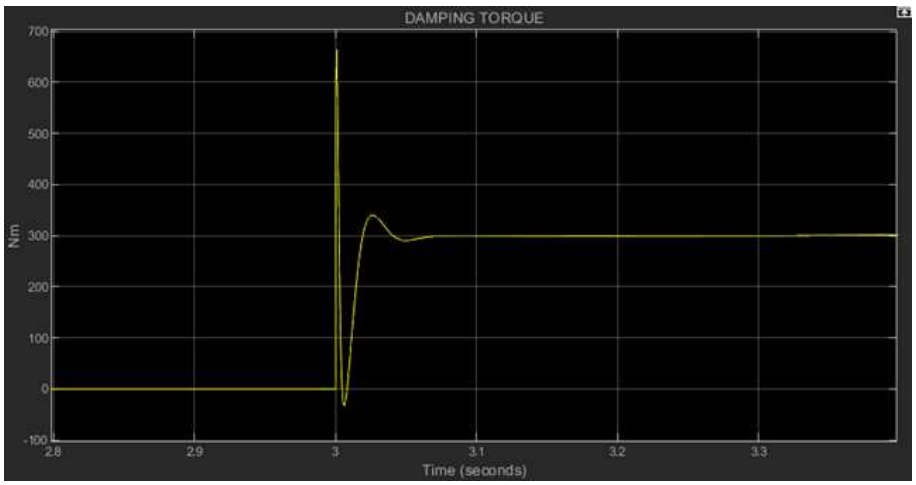

Figure 6.4. Damping torque contribution

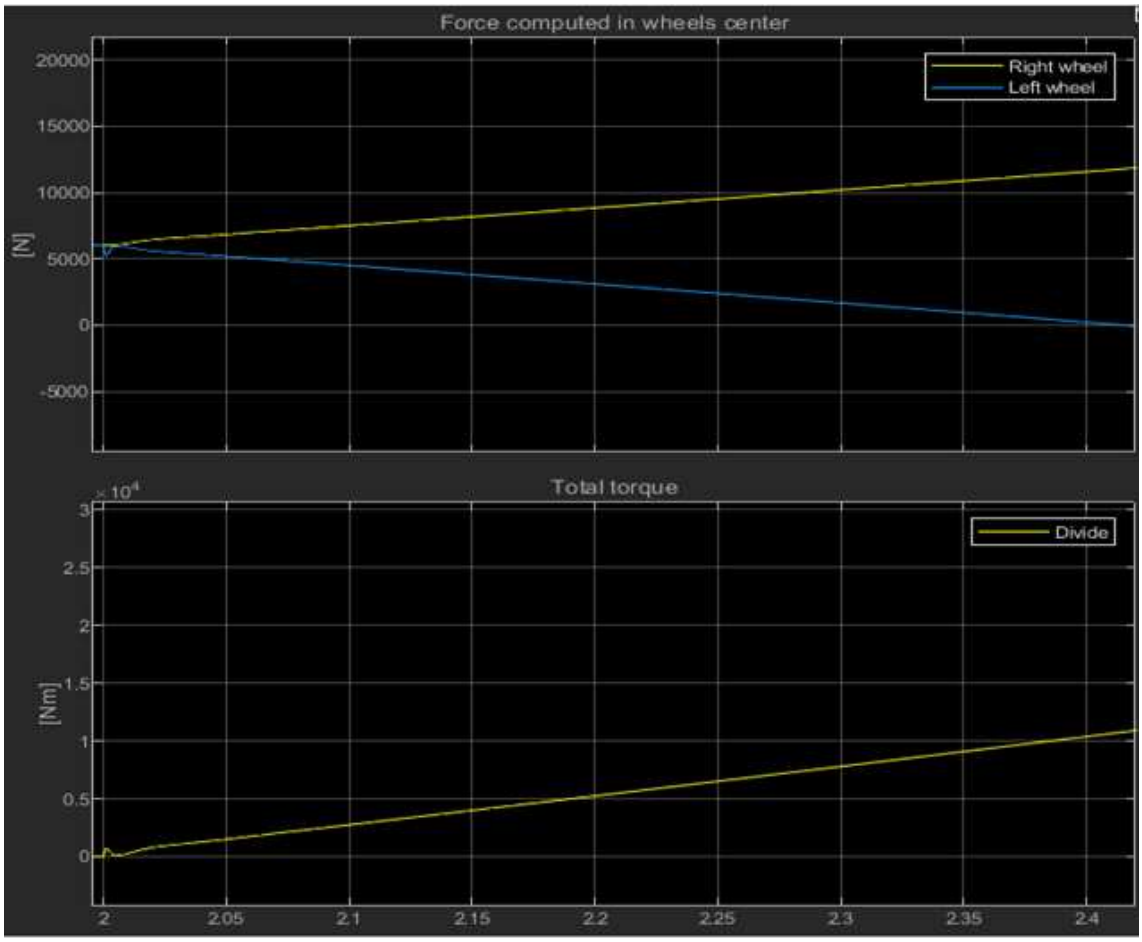

Figure 6.5. Total torque with angular velocity equal to 5 deg/s

Since the angular velocity and the torque are constant during the test, the damping coefficient is evaluated following the relation below:

$$c = \frac{T_{dam}}{\omega} \quad \left[\frac{Nm}{\frac{deg}{s}}\right] \tag{6.8}$$

In this case the torque is equal to $T_{dam} = 298N$ and $\omega = 5\ [deg/s]$, the resulting damping coefficient is $c = 49\ Nm/(deg/s)$; The damping coefficient can also be expressed in [Nm/(rad/s)], to do so it's necessary to convert angular velocity in rad/s, following the relation below:

$$\omega \quad \left[\frac{rad}{s}\right] = \omega \left[\frac{deg}{s}\right] * \frac{\pi}{180} \tag{6.9}$$

Several tests are performed applying different angular velocities, the results are listed in the next table: Analyzing the data shown in the table 6.2, it is possible to

TABLE 6.2

ω	DAMPING TORQUE	DAMPING COEFFICIENT	DAMPING COEFFICIENT
[deg/s]	[Nm]	[Nm/(deg/s)]	[Nm/(rad/s)]
0.5	9	18	1031,4
1	32	32	1833,6
1.5	59	39,3	2251,9
3	147	49	2807,7
5	298	59,6	3415,1
7.5	550	73,3	4202
10	855	85,5	4899,2
12.5	1230	98,4	5638,3
15	1650	110	6303

observe the increasing trend of the damping coefficient as the roll speed increases. Observing the time behaviour of the system in response to external input is possible to compute the rolling damping factor. The system is solicited by a lateral force step input applied to the car's COM. Then, the damping factor is evaluated by the logarithm decrement. The responce of the system is shown in figure 6.2

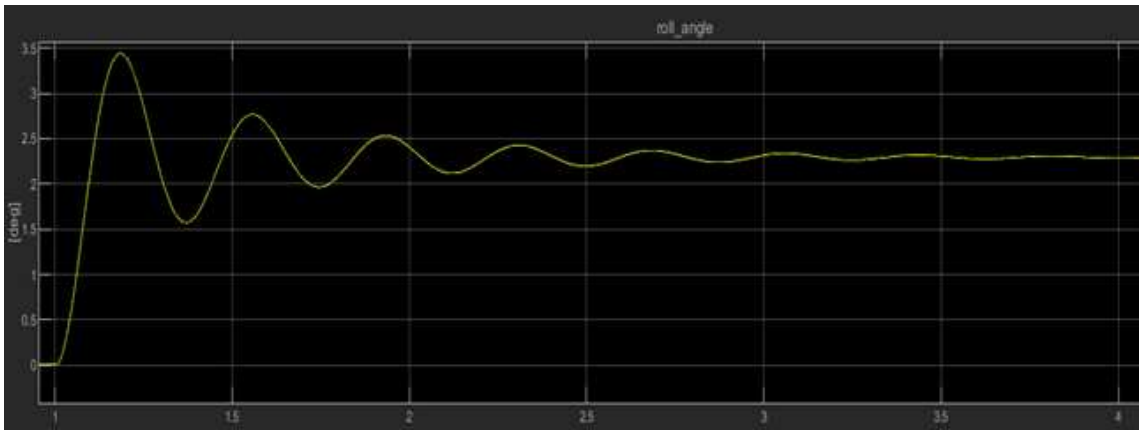

Figure 6.6. System responce to a lateral step force input of magnitude F=1.5*m*g

The results obtained in table 6.3 are represented in figure 6.2. It is important to stress that the damping ratio of the system is not constant but increases as the applied lateral force becomes bigger. By comparing the values referred to the

TABLE 6.3					
Lateral acceleration expressed in "g"	Logarithm decrement	damping factor	T	fn	fd
			[s]	[Hz]	[Hz]
0,2	0,596	0,094	0,374	2,68	2,67
0,4	0,662	0,105	0,374	2,69	2,67
0,5	0,694	0,11	0,374	2,69	2,67
0,75	0,764	0,121	0,374	2,69	2,67
1	0,815	0,129	0,374	2,70	2,67
1,25	0,855	0,135	0,373	2,71	2,68
1,5	0,887	0,14	0,371	2,72	2,69

natural and damped frequencies, table 6.3 and 6.1.1 in the case of roll and vertical damping, some considerations can be made: The frequency related to rolling behaviour is more constant with respect to the vertical one, however, the values are slightly higher.

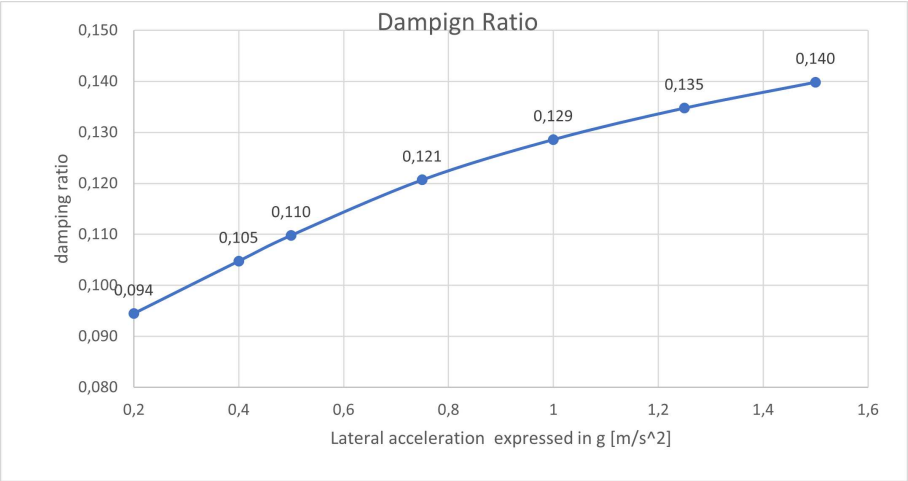

Figure 6.7. Damping ratio/lateral acceleration

Concluding, from observing the data collected in this chapter, it is clear the non-linearity of the system in roll conditions. However the results show. in figure **??** that the interconnected hydraulic system allows for an increase in the damping factor as the lateral acceleration step increases, so the vehicle becomes stiffer as the lateral acceleration becomes greater, these benefits handling performances

Chapter 7

Conclusions

The candidate carried out the Master's Degree Thesis project at "Manifattura Automobili Torino", where he was introduced to a new development project for an interconnected suspension system mounted in an SUV car,able to control roll angle without using an anti-roll bar.

The main object of this project is to study and understand the vertical and roll behaviour of the car, starting from the company request in terms of vertical and roll stiffness and to analyze the damping characteristics. Particular attention is reserved for the design and functioning of the hydraulic circuit, understanding how the internal components interact with the suspension behaviour.

The first chapter discusses the State of the art of the active, semi-active and anti-roll systems. The second chapter concerns the study and compares two working environments: Simulink and Multibody. The first one is a Mathematical approach, while the second one is geometrical. Both give good simulation results; however, since this project combines two domains (Mechanical and Hydraulic), Multibody is chosen to carry out the simulations and the required tests. The third chapter describes the modelling process and the rule followed to build the system using a Multibody environment. it is possible to study the scheme's geometry and its role in the system's dynamic behaviour. In fact, the characteristic dimensions of the suspension scheme are collected and recreated through CAD software, allowing to determine the roll centre and its kinematic characteristics. Eventually, in the last two chapters, several simulations are performed, such as parallel and opposite travel tests on the suspensions, to analyze the stiffness properties, and ride/handling tests to evaluate damping proprieties of the model. From the suspension scheme's kinematic studies carried out in chapter 4, it can be noticed that the roll angle of the car during a turn is almost completely transferred to the wheels camber angle, resulting in a bad handling configuration, however since the interconnected hydraulic circuit control the roll angle in an efficient way, this unwanted behaviour can be limited. The same configuration scheme allows the tyre to maintain a good

contact area if the sprung mass changes its height. The results presented in chapters 5 and 6 a good response in the vertical and lateral direction, proving that, the system discussed fulfils the vertical stiffness request given by the company and, in addition, provides good results in terms of roll behaviour. Same considerations can be made for the damping characteristic, which showed decent results in vertical analysis while, though it seemed to be less performing, in the roll behaviour. One of the main limits of this research is given by the non-correlation between the components dimensioned in the project and the real components taken from specialized catalogues, which may lead, in the future, to a non-correlation between simulation and real system behaviour

According to the analysis results, future studies can be carried out to optimize and improve the car's dynamic behaviour, starting by choosing different hydraulic components, for example, local resistance or gas-charged accumulator taken in catalogues or varying the suspension scheme.

Bibliography

[1] IEEE Simos A. Evangelou Member IEEE/ASME Carlos Arana, Member and ASME Daniele Dini, Member. Series active variable geometry suspension for road vehicles.

[2] H Du and N Zhang. Robust stability control of vehicle rollover subject to actuator time delay. 2008.

[3] Lorenzo Sisca Alessandro Messana Henrique de Carvalho Pinheiro, Francesco Russo. Active aerodynamics through active body control: Modelling and static simulator validation. 2020.

[4] Buma S Kamiya K Hirose M, Matsushige S. Toyota electronic modulated air suspension system for the 1986 soarer. In *Transactions on Industrial Electronics*.

[5] Zulkiffli Abd. Kadir Hishamuddin Jamaluddin Khisbullah Hudha, Fauzi Ahmad. Pid controller with roll moment rejection for pneumatically actuated active roll control (arc) suspension system. 2011.

[6] Kim JM Kim JS Ko DS KIM BM, JANG SB. Shock absorber for vehicle. 2013.

[7] Luca Castellazzi Sanjarbek Ruzimov Nicola Amati, Andrea Tonoli. Design of electromechanical height adjustable suspension. 2017.

[8] Streiter R. Active suspension system for a vehicle. 2001.

[9] Prabhakar D. Maskar Sagar B. Deshmukhpatil. Design optimization and analysis of composite automotive anti-roll bar. 2021.

[10] C. Spelta O. Sename L. Dugard S.M. Savaresi, C. Poussot-Vassal. In *Semi-Active Suspension Control Design for Vehicles*, pages 29–31, 2010.

[11] Gaurav Gaikwad Swaraj Kashid, Gaurav Parate. Adjustable pull-rod suspension system. 2021.

[12] Bauer W. Hydropneumatic suspension systems. 2010.

[13] Michel W. Height adjustment on a wheel suspension for motor vehicles. 2010.

[14] Michel W. Strut for a wheel suspension of motor vehicles. 2012.

[15] Els PS. Westhuizen SFVD. Slow active suspension control for rollover prevention. 2013.

[16] Haiping Du Xinxin Shao and Fazel Naghdy. Enhanced vehicle handling and ride through anti-pitch anti-roll hydraulically interconnected suspension. 2016.

List of Figures